Size and Frequency of Natural Forest Disturbances and the Amazon Forest Carbon Balance

Fernando D. B. Espírito-Santo[1,2,*], Manuel Gloor[3], Michael Keller[2,4,5], Yadvinder Malhi[6], Sassan Saatchi[1], Bruce Nelson[7], Raimundo C. Oliveira Junior[8], Cleuton Pereira[9], Jon Lloyd[3,10], Steve Frolking[2], Michael Palace[2], Yosio E. Shimabukuro[11], Valdete Duarte[11], Abel Monteagudo Mendoza[12], Gabriela López-González[3], Tim R. Baker[3], Ted R. Feldpausch[3], Roel J.W. Brienen[3], Gregory P. Asner[13], Doreen Boyd[14] and Oliver L. Phillips[3]

[1]NASA Jet Propulsion Laboratory, California Institute of Technology, Pasadena, CA 91109, USA
[2]Inst. for the Study of Earth, Oceans and Space, Univ. of New Hampshire, Durham, NH 03824, USA
[3]School of Geography, University of Leeds, Leeds, LS2 9JT, UK
[4]USDA Forest Service, International Institute of Tropical Forestry, San Juan, Puerto Rico
[5]Embrapa Monitoramento por Satélite, Campinas, SP, CEP 13070-115, Brazil
[6]School of Geography and the Environment, University of Oxford, Oxford, UK
[7] National Institute for Research in Amazonia (INPA), C.P. 478, Manaus, Amazonas 69011-970, Brazil
[8]Empresa Amazônia Oriental (CPATU), Santarém, PA, CEP 68035-110 C.P. 261, Brazil
[9]Belterra, PA, CEP 68143-000, Brazil
[10]Centre for Tropical Environmental and Sustainability Science (TESS) and School of Earth and Environmental Sciences, James Cook University, Cairns, Queensland 4878, Australia
[11]National Institute for Space Research (INPE), São José dos Campos, SP, CEP 12227-010, Brazil
[12]Jardin Botanico de Missouri, Oxapampa, Pasco, Peru
[13]Department of Global Ecology, Carnegie Institution for Science, Stanford, CA 94305, USA
[14]School of Geography, University of Nottingham, University Park, Nottingham, NG7 2RD, UK

Sep 26, 2013

*Author for Correspondence:

Fernando D.B. Espírito-Santo
NASA Jet Propulsion Laboratory
California Institute of Technology
Radar Science and Engineering Section
4800 Oak Grove Drive, MS 300-319
Pasadena, CA 91109

E-mail: f.delbon@gmail.com

Studies of the atmospheric accumulation of anthropogenic CO_2 indicate a large terrestrial carbon sink in recent decades[1–5], with a substantial fraction located in intact tropical forests[6,7]. Evidence for a tropical sink[5,8,9] is supported by data from forest inventory plots. However, the plot network has been criticized for its failure to represent landscape-scale processes[10–13] and especially the effect of severe natural disturbances[9–12,14]. We characterize for the first time the frequency distribution of disturbance events in natural forests [9,11–13] from 0.01 ha to 2,651 ha size throughout Amazonia using a novel combination of forest inventory, airborne LiDAR, and satellite passive optical remote sensing data. We find that small-scale mortality events are responsible for aboveground biomass losses of about 1.6 Pg C y^{-1} over the entire Amazon region, intermediate-scale disturbances for about 0.25 Pg C y^{-1}, and with the largest-scale disturbances by blow-downs only accounting for about 0.004 Pg C y^{-1}. Simulation of growth and mortality based on the forest census growth rates and the region-wide disturbance frequency distribution indicates that even when all carbon losses from local and landscape-scale disturbances are considered these are outweighed by the net biomass accumulation by tree growth, supporting the inference of an Amazon wide carbon sink.

Global records of atmospheric CO_2 concentrations, fossil fuel emissions, and ocean carbon uptake estimated based on ocean surveys indicate that there is a large terrestrial carbon sink[2,6] of which a substantial portion may be due to uptake by old growth tropical forests[15]. On the other hand, were some of the current large tropical forest carbon pools (including ~100 Pg C in aboveground biomass in Amazonia[16,17]) to be released rapidly to the atmosphere[10], it would substantially enhance greenhouse warming[2]. Understanding the nature and trajectory of the Amazon forest carbon balance is therefore of considerable importance.

The evidence for a tropical old-growth forest sink is based primarily on repeated biometric measurements of growth and death of individual trees across the tropics. These measurements indicate that at the plot-level old-growth forests in Amazonia and Africa have apparently gained carbon over the last 30 years[4,5,8,9]. The extrapolation of regional trends from a relatively small number of ~1-ha sized plots has been questioned because potentially unsampled natural disturbances at the landscape-scale could counterbalance tree level growth[11,12]. Resolving this issue requires assessing whether estimates of biomass gain are robust when fully considering disturbances of all sizes[14,18]; we test this statistically against the null hypothesis of net zero change in biomass. Here we synthesize and characterize for the first time the frequency distribution of natural disturbance at all spatial scales across forests of the Amazon region using a combination of forest censuses, airborne LIDAR and passive optical remote sensing from satellite. We ask whether the net biomass gains inferred from forest census data are an artifact of the small size (~1 ha) and limited number of plots in the plot network[9]. We address this question using a simple stochastic forest simulator based on growth statistics from the forest census network and the new regional disturbance size-frequency distribution.

Our approach includes natural causes of tree mortality[14] (including partial mortality such as branch falls) that liberate carbon[10], but excludes anthropogenic disturbance caused by forest clearing, logging, and fires[1,2]. To determine the frequency distribution of natural disturbances in the Amazon at all scales, we quantify small area disturbances using records of (*i*) biomass losses from a long-term repeat measurement network spatially distributed across the entire Amazon[3–5,9,19] supplemented by (*ii*) two large forest plot surveys (53 and 114 ha) in the Eastern Amazon[20], intermediate area disturbances using (*iii*) tree-fall gaps detected by airborne LiDAR from four large surveys (48,374 ha) in Southern Peru[21], and large area disturbances from blow-downs using data sets[22,23] from Landsat satellite images in (*iv*) an East-West[22] transect and (*v*) for the entire Brazilian Amazon forest[23]. For small area disturbances we estimate biomass loss associated with area loss of each event of disturbance. For intermediate disturbances several assumptions are required to translate the measurements of forest structure from ~1 m airborne LiDAR data into an estimate of biomass loss (see Supplementary Material). To ensure that our test of the hypothesis that the plot network effectively measures biomass change is as robust as possible, our assumptions conservatively err on the generous side to the magnitude and frequency of intermediate disturbance. For large disturbances, we reanalyzed records of blow-downs likely caused by downdrafts associated with convective clouds[24] covering Brazilian Amazon forests[23] using historical Landsat satellite images (pixels sizes ~30 m) and a more recent East-West mosaic of Landsat scenes covering a portion of the Amazon[22]. Combining the spatial records of large disturbances detected by Landsat[22,23] with a recently developed map of aboveground biomass[17], we estimate carbon loss associated with these large disturbances (Fig. 1). Because of the uncertainties associated with below-ground biomass[1,2,6,17], we discuss carbon losses only in terms of aboveground biomass (AGB) which probably accounts for ~80% of live biomass in Amazonia[1,16,17].

For determining the largest blow-downs we build on an earlier study of large natural disturbances[23] which identified 330 blow-downs ≥ 30 ha distributed in 72 Landsat scenes from the total 137 scenes (Supplementary Fig. S5) acquired between 1988 and 1991 across the ~3.5×10^6 km^2 forested area of the Brazilian Amazon[25]. Subsequent digital image processing for blow-down detection[22] in the Central Amazon collected around the year 2000 (27 Landsat scenes) further revealed a substantial number of medium sized blow-downs (5-30 ha) not detected using earlier visual inspection methods[23]. In both studies[22,23] spatial analysis showed a high concentration of all detected blow-down disturbances west of ~58^o W clearly associated with areas of strong convective activity[24] as measured from cloud-top temperatures from the TRMM satellite[22]. Reanalyzing that data[23] here using a Gaussian kernel smoothing algorithm for cluster analysis[26] confirms the concentration of blow-down disturbances in the western Amazon (Fig. 2) with blow-downs 12 times more frequent west of 58^o W than to the east. This conclusion does not depend on the bandwidth size used for the cluster analysis (Supplementary Fig. S6, S7 and S8).

Amazon-wide there are thus two spatially disjoint size and severity domains of large disturbances: one domain with large blow-downs centered west of Manaus and another one where the largest blow-downs are absent (Fig. 2). Although it has been suggested that the disturbance size frequency distribution follows a power law $p(x) \propto x^{-\alpha}$ (probability density *p(x)* and size of an event *x*)[27], the observed distribution suggests a more subtle picture (Fig. 3). Visually three sections may be identified: an approximately exponential decline of frequency with size for smallest size disturbances, a power law type decline for intermediate scales and another power law decline for the largest-scale disturbance blow-downs (Fig 3a,c). The power law decline for intermediate disturbances with size appears to be steeper than for largest blow-downs. This is seen in the estimated return times versus disturbance severity relationship (see Methods) that reveals a sharp increase to higher values for intermediate range disturbances from 1 to 10 ha (Fig. 3b,d). The data also show that disturbance-induced tree mortality that cause small-area disturbances have a return time of about 100 years (Fig. 3b,d). This agrees with studies from other tropical forest regions that observed an annual tree-fall disturbance rate of 1% by the process of gap formation due to tree death[28]. By contrast, the return time of large blow-downs is very long -- that is, such events are extremely rare -- ranging from 4×10^5 y to greater than 10^7 y depending on size (Fig. 3b). Small disturbances (<0.1 ha) per year are many orders of magnitude more frequent (~10^6 events) than large blow-downs (~10^3 events) over the Amazon (Fig. 3b).

Based on the size and frequency of natural disturbances of our data scaled to all Amazon forest areas (~6.8 x 10^8 ha)[24], the total carbon released by natural disturbances is estimated as 1.88 Pg C y^{-1}, where approximately 1.66 Pg C y^{-1} or ~88.3% is accounted for by small-scale mortality (< 0.1 ha), ~12.7% from intermediate (0.1 to 5 ha), and ~0.02% from large disturbances (> 5 ha). Large disturbances although visually impressive are extremely rare (Fig. 3b,d), and the estimated amount of biomass loss is only 0.004 Pg C y^{-1}. By comparison net carbon emissions caused by forest clearing in the Brazilian Amazon[1] in the 1990's were ~0.2 Pg C y^{-1}. Conversion of the mortality to approximate Amazon forest areas implies that natural mortality affects 2.0 x 10^7 ha y^{-1} or 2% of total forest area, where about 80.0% is from small-scale mortality, ~19.9% is from intermediate and only 0.1% from large disturbances.

The estimated disturbance spectrum permits us to address whether the observed carbon balance of the Amazon tropical forests inferred from forest plot censuses does indeed significantly reflect carbon gain (carbon accumulation rates are significantly greater than zero) considering the potential of disturbance to negate this finding[18]. For this purpose we use a stochastic forest growth simulator[9] of the form $dM = G \times dt - D \times dt$, where dM is aboveground forest biomass loss in units of carbon per area, dt a time interval, here one year, and G and D stochastic variables distributed according to the observed distributions of aboveground mass gain due to growth (G) and loss (D) due to mortality[9,11,13] (for details please see below). We use the simulator (Supplementary Fig. S11) to assess the mean net carbon balance and its standard deviation we simulated 10^9 equivalent annual observations of each scenario and, statistical significance of the results is assessed using a *t-test* (Tab. 1). The scenario that we consider to be most realistic for the whole Amazon region is marked bold in Table 1. For all scenarios ensemble mean net gains are positive and for all but the most extreme scenario, the *t-tests* reveal significance. Intermediate disturbances have a notable effect on mean with relatively small effect on the variance. In contrast, large disturbances have no perceptible effect on the mean while greatly increasing the variance and therefore the probability of detection for a positive biomass trend. The exceptional scenario -- which given our data are clearly over-pessimistic -- assumes the largest blow-downs occurring not only in Central Amazonia but throughout the Amazon forest regions and intermediate disturbances occurring at a rate that greatly over-represents the importance of floodplain forests (Supplementary Tab. 2S).

In summary, we have characterized for the first time the full size distribution and return frequency of natural forest mortality and disturbance in the Amazon forest biome (Fig. 3). Our findings help to resolve the debate about the relative importance of intermediate- and larger-area disturbances[9,11–13] and gains in biomass stocks in intact tropical forest plots[9] for determining the regional-scale carbon balance. In our simulation taking into account the full range of natural disturbances, we find significant increases in the biomass of intact Amazonian forest. Although the simulation does not consider the spatial and temporal interactions of growth and disturbance, these results nonetheless imply that natural disturbance processes in Amazonia are insufficiently intense or widespread to negate the conclusion from the pan-Amazon plot network that old-growth forests in that region have gained biomass. Uncertainty about the role of disturbances in affecting estimates of the long-term trajectory of the carbon balance of tropical forests is declining as the forest monitoring effort on the ground increases both in time and space[4,5,9,19]. Our characterization of the natural disturbance regime of the Amazon forest yields new insight into the role of disturbance in tropical forest ecology and carbon balance.

Methods Summary

Forest Inventories and Remote Sensing to Assess Disturbance Effective detection of forest disturbance that results in tree mortality[4,6,11–13,20] and the release of carbon to the atmosphere[1,2,6,10] requires observational methods that encompass relevant spatial scales[2,14]. We combine repeat measurement data from forest censuses with analysis of Landsat and LiDAR images permitting us effectively to estimate mortality across all relevant spatial scales (Fig. 1). For mortality that affects less than about 0.1 ha, we combine two spatial and temporal sources of data: (1) 484 forest plot censuses from 135 (~1 ha) permanent plots covering 1545 census years of tree-by-tree measurements, distributed over the entire Amazon region including the Guiana Shield (see Supplementary Methods), from the RAINFOR network which covers 45 Amazon regions[9]; and (2) losses of biomass in areas of branch or tree-fall gaps[10,11,28] of two plots of 53 and 114 ha from the Tapajós National Forest in the Eastern Brazilian Amazon[20]. To estimate disturbances at an intermediate area (from 0.1 to 5 ha) we used a large area of airborne LiDAR data from four samples in the Southern Peruvian Amazon[21] covering in total 48,374 ha. For disturbances covering large areas (disturbance size > 5 ha) we combine three remote sensing data sets: (1) a spatially extensive record of large disturbances from blow-downs ≥ 30 ha from 128 Landsat scenes from the Brazilian Amazon and 8 scenes from outside of Brazil[23]; (2) a high resolution study of blow-downs ≥ 5 ha using 27 Landsat scenes on an east-west transect in the central Amazon[22]; and (3) a multi-sensor remote sensing product of aboveground biomass for the tropics[17]. For all mortality (Tab. 1; Supplementary Tab. S1) we estimate areas and biomass defined as losses in aboveground biomass (AGB) stocks (Supplementary Fig. S3).

Return time versus disturbance size To estimate return times of forest area loss events of a given size we first scale estimated number frequencies to the full Amazon forest by multiplying them with the ratio (A_{Amazon}/A_{probed}) where A_{Amazon}= 6,769,214 km^2 (INPE[25], Supplementary Fig. S4) is the total forested area of the Amazon. The empirical probability $p^*(A)\Delta A$ that a fixed location will be affected by a disturbance of area A during one year is then $p^*(A)\Delta A = ((\sum_{A' \in (A, A+\Delta A)} A')/A_{Amazon})$ where the sum is over all events across the Amazon region with area A' in the interval $(A, A+\Delta A)$, and ΔA is a finite area interval. The probability for the occurrence of a disturbance event per year with area loss larger than A at a fixed location is then

$$P(X \geq A) = \sum_{A' \geq A}^{\infty} p^*(A')\Delta A' = \frac{A_{total}^{disturbed}}{A_{Amazon}} - \sum_{A'=0}^{A} p^*(A')\Delta A'$$ using the identity

$$\sum_{A=0}^{\infty} p^*(A)\Delta A = \frac{1}{A_{Amazon}} \sum_{i=1}^{N} A_i = \frac{A_{total}^{disturbed}}{A_{Amazon}}$$ (i.e. not 1, therefore the notation p^* instead of p)

where N is the total number of observed disturbances and $A_{tot}^{distrbd} = \sum_{i=1}^{all\ disturbance} A_i$ is the total annually disturbed forest area in the Amazon.

Therefore an estimate for the return time $\tau(X \geq A)$ of a disturbance event X with forest area lost larger than A at a fixed location is given by the inverse of the cumulative PDF:

$$\tau(X \geq A) = \frac{1}{P(X \geq A)} = \frac{1}{\frac{A_{total}^{disturbed}}{A_{Amazon}} - \sum_{A'=0}^{A} p^*(A')\Delta A'}.$$

An analogous equation holds for return time with respect to biomass loss associated with a disturbance event.

Forest Aboveground Biomass Simulation Once the disturbance spectrum of aboveground biomass loss is defined we can infer the standard deviation introduced into an ensemble of growth rates from forests censuses using the simple stochastic forest simulator of the form $dM = G \times dt - D \times dt$ introduced above which predicts forest carbon mass change per area (M) due to growth (G) and loss (D) due to mortality[9,11,13] during the time interval dt. For G we used as input parameters growth from 484 forest censuses[9] covering N=135 plots and N = 1545 census years, and mortality (aboveground biomass loss) from our new disturbance spectrum analysis. To generate random numbers distributed according to our observed distribution we use the inverse transform method[9]. For growth we use specifically $G \sim N(\mu,\sigma)$ with $\mu = 2.5$ or 2.75 (Mg C ha^{-1} yr^{-1}) respectively, and $\sigma = 0.85$ (Mg C ha^{-1} yr^{-1}), the mean value for the Amazon region according to the RAINFOR data[9] and Eastern Amazon respectively. For D, we used our Amazon forest mortality frequency distribution (Fig. 3) and modifications thereof for purpose of sensitivity and uncertainty analysis of our approach (see main text and legend of Tab. 1 and Supplementary Tab. S2). The growth component of the simulation model is conservative with respect to the hypothesis of net biomass gains, as it neglects any growth enhancement after large disturbance events[29] and so overestimates the period of biomass decline. In real forests, disturbance-recovery growth enhancements shorten the total period for which disturbance-induced net biomass losses occurs for any given patch of forest, and therefore mitigate the impact of disturbance events on the summary statistics of net biomass trajectories.

To ensure that the simulation of disturbances is operating correctly we checked the predicted Amazon disturbance spectrum against the observed spectrum using a sample of 5×10^8 simulation runs, also revealing that such a number is sufficient to reproduce the full spectrum. The simulator was then run for 10^9 annual equivalent samples for each scenario (Tab. 1, Supplementary Tab. S2, and S11). We started the simulator from an arbitrary value zero and let mass accumulate or decline indefinitely thus, in effect, permitting to represent the whole Amazon. From these 10^9 samples of biomass gain or loss we assessed whether the inference of a large carbon sink in old-growth forests is statistically significant[9], by consulting the *t* statistic $t = \overline{dM/dt}/(\sigma/\sqrt{N})$. $\overline{dM/dt}$ is the trajectory sample mean net carbon balance over one year, and σ the trajectory sample standard deviation over the same period. A *t-test* is justified given the large sample size despite the skewed distributions of net gains, i.e. means are indeed nearly normally distributed as predicted by the central limit theorem and tested by Monte Carlo simulations based on the observed distribution of net gains.

We run the simulator for various disturbance distribution scenarios to explore the sensitivity of the model to parameter selection. Scenarios with results summarized in Table 1 include (*i*) three blow-down extents: none, Central Amazon, and the full region, and (*ii*) two assumed time-scales (1 and 3.6 y) for detectability of disturbances observed with LiDAR[21]. Sensitivity to change in growth rates and an extreme case intermediate disturbance regime taken from the Peruvian river floodplains are also examined (Supplementary Tab. S2). The two intermediate disturbance area cases explore the sensitivity of our results to the spatially biased coverage of the LiDAR data to one part of the southwest Amazon. The first of the intermediate-scale scenarios use data from *terra firme* only, the most relevant data for answering our main question because *terra firme* forests occupy a far larger portion of the Amazon region than seasonally flooded forests. The second extreme intermediate-scale scenario includes also LiDAR data from flooded forests, which has a greater frequency of larger area disturbance, presumably fluviallyinduced although the effect of human disturbance cannot be categorically eliminated because the region studied is affected by extensive largely unregulated placer gold mining. For small and large area disturbances, we did not differentiate geomorphic regimes because they were not apparent in the data.

Acknowledgements This research was supported by the NASA Earth System Science Fellowship (NESSF) Grant # NNX07AN84N (F.E-S. and M.K.), the NASA Terrestrial Ecology Program contribution to the Large Scale Biosphere-Atmosphere Experiment in the Amazon (LBA), CalTech Postdoctoral Fellowship at JPL (F.E-S.), NERC consortia projects, AMAZONICA (NE/F005806/1, TROBIT) for support of RAINFOR and M.G., R.B., O.P., T.F., G.L., J.L., and Y.M., an Advanced Grant from the European Research Council (T-FORCES, O.P.). We thank the Brazilian Ministry of Science and Technology for its support of the LBA program and the National Institute for Amazon Research for implementation of this program. Development of the RAINFOR network including measurement of biomass dynamics has been supported by 34 different grants. We thank in particular the Gordon and Betty Moore Foundation, and the authorities in Bolivia, Brazil, Colombia, Ecuador, Guyana, Peru and Venezuela, and colleagues across the region for support. The manuscript has benefitted form discussions with Simon Lewis and comments from three anonymous reviewers. We are grateful to Dr. Jeff Chambers who brought several of us together in an excellent meeting in 2006 at Tulane University where the idea for quantifying the disturbance spectrum was born. The Carnegie Airborne Observatory is made possible by the Gordon and Betty Moore Foundation, the Grantham Foundation for the Protection of the Environment, the John D. and Catherine T. MacArthur Foundation, the Avatar Alliance Foundation, the W. M. Keck Foundation, the Margaret A. Cargill Foundation, Mary Anne Nyburg Baker and G. Leonard Baker Jr., and William R. Hearst III.

Author Contributions M.K., M.G., O.P. and Y.M. conceived this study. F.E-S, M.K., M.G., O.P., Y.M. designed the research study. F.E-S. integrated all data sets. F.E-S. and M.G. calculated and analyzed the data. M. G. created the stochastic simulator, ran the simulations and produced the regional frequency and return time distributions. S.S. helped with the data input layer of blow-down carbon biomass losses. B.N. and F.E-S. produced the regional map of blow-downs and provided all information for the spatial analysis. F.E-S., R.C.O. and C.P. collected the data of the large plots (114 and 53 ha) at Tapajós National Forest, Brazil. Y.E.S and V.D. produced the remote sensing layers of undisturbed forest of South America. O.P., J.L., S.F., M.P. and all others authors helped with the review and suggestions. A.M., G.L-G., T.B., T.F., R.B., and O.P. led and analyzed more recent RAINFOR campaigns. G.A. provided and helped with the LiDAR data from Peru. F.E-S., M.G., M.K. and O.P. wrote the paper.

Additional Information Correspondence and requests for material should be addressed to F.E-S. (f.delbon@gmail.com).

References

1. Houghton, R. A. *et al.* Annual fluxes of carbon from deforestation and regrowth in the Brazilian Amazon. *Nature* **403,** 301–304 (2000).

2. Schimel, D. S. *et al.* Recent Patterns and Mechanisms of Carbon Exchange by Terrestrial Ecosystems. *Nature* **414,** 169–172 (2001).

3. Phillips, O. L. & Gentry, A. H. Increasing turnover through time in tropical forests. *Science* **263,** 954–958 (1994).

4. Phillips, O. L. *et al.* Changes in the carbon balance of tropical forests: evidence from long-term plots. *Science* **282,** 439–442 (1998).

5. Lewis, S. L. *et al.* Increasing carbon storage in intact African tropical forests. *Nature* **457,** 1003–U3 (2009).

6. Sarmiento, J. L. *et al.* Trends and regional distributions of land and ocean carbon sinks. *Biogeosciences* **7,** 2351–2367 (2010).

7. Pan, Y. D. *et al.* A Large and Persistent Carbon Sink in the World's Forests. *Science* **333,** 988–993 (2011).

8. Phillips, O. L. *et al.* Drought Sensitivity of the Amazon Rainforest. *Science* **323,** 1344–1347 (2009).

9. Gloor, M. *et al.* Does the disturbance hypothesis explain the biomass increase in basin-wide Amazon forest plot data? *Global Change Biology* **15,** 2418–2430 (2009).

10. Körner, C. Slow in, rapid out - Carbon flux studies and Kyoto targets. *Science* **300,** 1242–1243 (2003).

11. Fisher, J., Hurtt, G., Thomas, Q. R. & Chambers, J. C. Clustered disturbances lead to bias in large-scale estimates based on forest sample plots. *Ecology Letters* **11,** 554–563 (2008).

12. Chambers, J. Q., Negrón-Juárez, R. I., and Hurtt, G. C., Marra, D. M. & Higuchi, N. Lack of intermediate-scale disturbance data prevents robust extrapolation of plot-level tree mortality rates for old-growth tropical forests. *Ecology Letters* **12,** E22–E25 (2009).

13. Lloyd, J., Gloor, E. U. & Lewis, S. L. Are the dynamics of tropical forests dominated by large and rare disturbance events? *Ecology Letters* **12,** E19–E21 (2009).

14. Frolking, S. *et al.* Forest disturbance and recovery: A general review in the context of spaceborne remote sensing of impacts on aboveground biomass and canopy structure. *Journal of Geophysical Research-biogeosciences* **114,** G00E02 (2009).

15. Grace, J. *et al.* Carbon-Dioxide Uptake by an Undisturbed Tropical Rain-Forest in Southwest Amazonia, 1992 to 1993. *Science* **270,** 778–780 (1995).

16. Malhi, Y. *et al.* The regional variation of aboveground live biomass in old-growth Amazonian forests. *Global Change Biology* **12,** 1107–1138 (2006).

17. Saatchi, S. S., Houghton, R. A., Alvala, R. C. D. S., Soares, J. V & Yu, Y. Distribution of aboveground live biomass in the Amazon basin. *Global Change Biology* **13,** 816–837 (2007).

18. Chambers, J. Q. *et al.* The steady-state mosaic of disturbance and succession across an old-growth Central Amazon forest landscape. *Proceedings of the National Academy of Sciences* **110,** 3949–3954 (2013).

19. Malhi, Y. *et al.* An International Network to Monitor the Structure, Composition and Dynamics of Amazonian Forests (Rainfor). *Journal of Vegetation Science* **13,** 439–450 (2002).

20. Espírito-Santo, F. D. B. *et al.* Gap formation in large forest plots of Brazilian Amazon: Effects on carbon cycling and measurement using high resolution optical remote sensing. *Plant Ecology and Diversity* (2013). doi:10.1080/17550874.2013.795629

21. Asner, G. P. *et al.* Forest Canopy Gap Distributions in the Southern Peruvian Amazon. *PLoS ONE* **8,** e60875 (2013).

22. Espírito-Santo, F. D. B. *et al.* Storm intensity and old-growth forest disturbances in the Amazon region. *Geophysical Research Letters* **37,** L11403 (2010).

23. Nelson, B. W. *et al.* Forest disturbance by large blowdowns in the Brazilian Amazon. *Ecology* **75,** 853–858 (1994).

24. Garstang, M., White, S., Shugart, H. H. & Halverson, J. Convective cloud downdrafts as the cause of large blowdowns in the Amazon rainforest. *Meteorology and Atmospheric Physics* **67,** 199–212 (1998).

25. INPE. *Instituto Nacional de Pesquisas Espaciais, PRODES (Projeto de Desflorestamento da Amazônia)*. (2011).

26. Ripley, B. D. *Spatial statistics*. 132 (John Wiley & Sons, 1981).

27. Solé, R. V & Manrubia, S. C. Are Rainforests Self-Organized in a Critical State? *Journal of Theoretical Biology* **173 ,** 31–40 (1995).

28. Whitmore, T. C. Canopy gaps and the two major groups of forest trees. *Ecology* **70,** 536–538 (1989).

29. Chambers, J. Q. *et al.* Response of tree biomass and wood litter to disturbance in a Central Amazon forest. *Oecologia* **141,** 596–611 (2004).

30. Hubbell, S. P. & Foster., R. B. in *Plant Ecology* (Crawley, M.) 77–95 (Blackwell, Oxford, UK, 1986).

Table 1. Summary of Amazon forest disturbance simulator results and statistical significance of simulated mean aboveground biomass gains for a range of scenarios. We vary (1) occurrence of large-disturbance blow-downs[22,23], i.e. the large-end tail of the disturbance frequency distribution, and (2) age of intermediate-range disturbances. For (1) we distinguish three cases: (*i*) no large-disturbance blow-downs[22,23], blow-downs as observed (*ii*) only in central Amazon (~20% of the Amazon region), (*iii*) everywhere in the Amazon with the same frequency of events as in the Central Amazon (i.e. in total there are 5 times more large-area events). For (2) we distinguish intermediate-range disturbances occurring across the entire Amazon region distributed according to LiDAR surveys[21] (plots 1,4,5 and 12) of erosional terra firme (ETF) forests (33,196 ha) between a mean gap age of 1 and 3.6 years based on gap closure observations of a 50 ha plot on Barro Colorado Island[30]. We assumed an annual mean mass gain[5,8,9] of 2.5 Mg C ha^{-1} yr^{-1} in areas of *terra firme* forests. The simulator of forest mortality is based on the frequency distribution of disturbance area. To convert area losses to biomass losses we assumed a forest mass density of 170 Mg C ha^{-1} for all simulations, a high value and nearly 50% greater than the LiDAR landscape used to estimated intermediate disturbance dynamics[5,8]. Assessment of each scenario is based on a set of 10^9 annual equivalent samples. Significance is assessed with a *t*-test considering $t_{\mathrm{sim}} = (dM/dt)/(\sigma/\mathrm{sqrt}(N))$ where dM/dt is ensemble mean mass gain (Mg C ha^{-1} y^{-1}), σ the standard deviation of the mass gain distribution and N the number of observations. For N we use either conservatively $N = 135$ the total number of observational plots or $N = 1545$, the total number of plot census years reflecting the stochastic nature of disturbance and therefore the near independence of plot results from year-to-year. Gain results are statistically significant at the 95% level if $t_{\mathrm{sim}} \gtrsim t_{\{0.975,\mathrm{N}=135\}} \approx t_{\{0.975,\mathrm{N}=1545\}} = 1.96$ and at the 99% level if $t_{\mathrm{sim}} \gtrsim t_{\{0.995,\mathrm{N}=135\}} \approx t_{\{0.995,\mathrm{N}=1545\}} = 2.58$. The most credible results are highlighted in bold.

Assumed annual mean mass gains[5,8,9]: 2.5 Mg C ha^{-1} yr^{-1} and intermediate-scale disturbances[12,13] modeled with:

Intermediate-Scale Disturbances	Large-Scale Blow-downs[22,23]		
LiDAR data[21] from terra firme (gaps age[30] ~ 1 yr old)	None	Central Amazon	All Amazon Region
dM/dt*	-	0.85	-
σ*	-	4.40	-
t_{obs}(N=135)	-	2.24	-
t_{obs}(N=1545)	-	7.59	-
LiDAR data[21] from terra firme (gaps age[30] ~ 3.6 yr old)			
dM/dt*	0.94	**0.94**	0.94
σ*	2.19	**3.77**	12.4
t_{obs}(N=135)	4.99	**2.90**	0.88
t_{obs}(N=1545)	16.9	**9.80**	2.98

Figure Captions

Figure 1. Amazon Basin-wide data of natural forest disturbances. Spatial distribution of RAINFOR forest census plots[9] (n=135), inspected Landsat images (n=137) with occurrences of large blow-down disturbances ≥ 30 ha[22] (n=330 blow-downs) and ≥ 5 ha[21] (n=279 blow-downs) underlain by an aboveground biomass map of the Amazon (a). Large forest inventory plot of 114 ha[19] with canopy gaps (n=55) overlain on a high resolution IKONOS-2 image acquired in 2008 in the Eastern Amazon (b). Large plot of 53 ha[19] with canopy gaps (n=51) over a second high resolution IKONOS-2 image acquired in 2009 (c). Digitally classified blow-downs in an East-West mosaic of Landsat images from central Amazon (d). Representation of disturbance size areas found in all Landsat images - blow-downs disturbances ≥ 30 ha areas are proportional to the size of the circles (e). Location of the LiDAR airborne campaigns in the Southern Peruvian Amazon[20] (f). LiDAR data collections in 5 large transects of tropical forest (48,374 ha, n=30,130 gaps > 20 m^2 in erosional terra-firme and depositional forests) (g). Details of the detection of gaps in LiDAR canopy height model (CHM) - 2 m height threshold[30] were used to detect tree-fall gaps in CHM (h). White, blue, black and red lines on the map (a) indicates Brazilian border, the mosaic of Landsat images in Central Amazon[21], Landsat scenes in all Brazilian Amazon[22] and the LiDAR airborne campaigns in Peru[20], respectively.

Figure 2. Spatial distribution of large disturbances in the Brazilian Amazon. Cluster map of blow-downs of Brazilian Amazon using a Gaussian smoothing kernel[25] with bandwidth of 200 km modeled from 330 large disturbances ≥ 30 ha detected in 137 Landsat images over the Amazon region[22]. Color bar is the intensity of large disturbances in the Amazon (number of blow-downs per km^2).

Figure 3. Estimated frequency distributions of natural forest disturbances in the Amazon. Number of disturbances per year obtained by scaling observed events to the full Amazon region by multiplication with the inverse of observed area fraction (a), Number of disturbances per year and per histogram bin-width, with bin-widths chosen such as to

include at least one event; this distribution is linearly proportional to *p(x)* of Δlog (number of occurrences)/Δlog (disturbance size) ≈ -2.5, and (b), return times versus severity of events calculated using the inverse of the cumulative PDF (see Methods) for various combinations of the data from repeated plot measurements, LiDAR surveys and Landsat imagery. For panels (a) and (b) largest blow-downs (those detected by Landsat imagery) are scaled to the region by multiplication of Amazon area fraction with large blow-downs. Panels (c) and (d) are similar to (a) and (b) but with respect to disturbance biomass loss instead of disturbance area. In panels (b, d) solid lines correspond to the case where large blow-downs are included only in the Central Amazon while the dashed lines correspond to the case where largest blow-downs are assumed to occur everywhere in the region (as a sensitivity study) and similarly the dashed light blue line corresponds to the case where also floodplain LiDAR data with river-driven disturbances are included (note that the forest plot network is based overwhelmingly on non-floodplain plots).

Figure 1

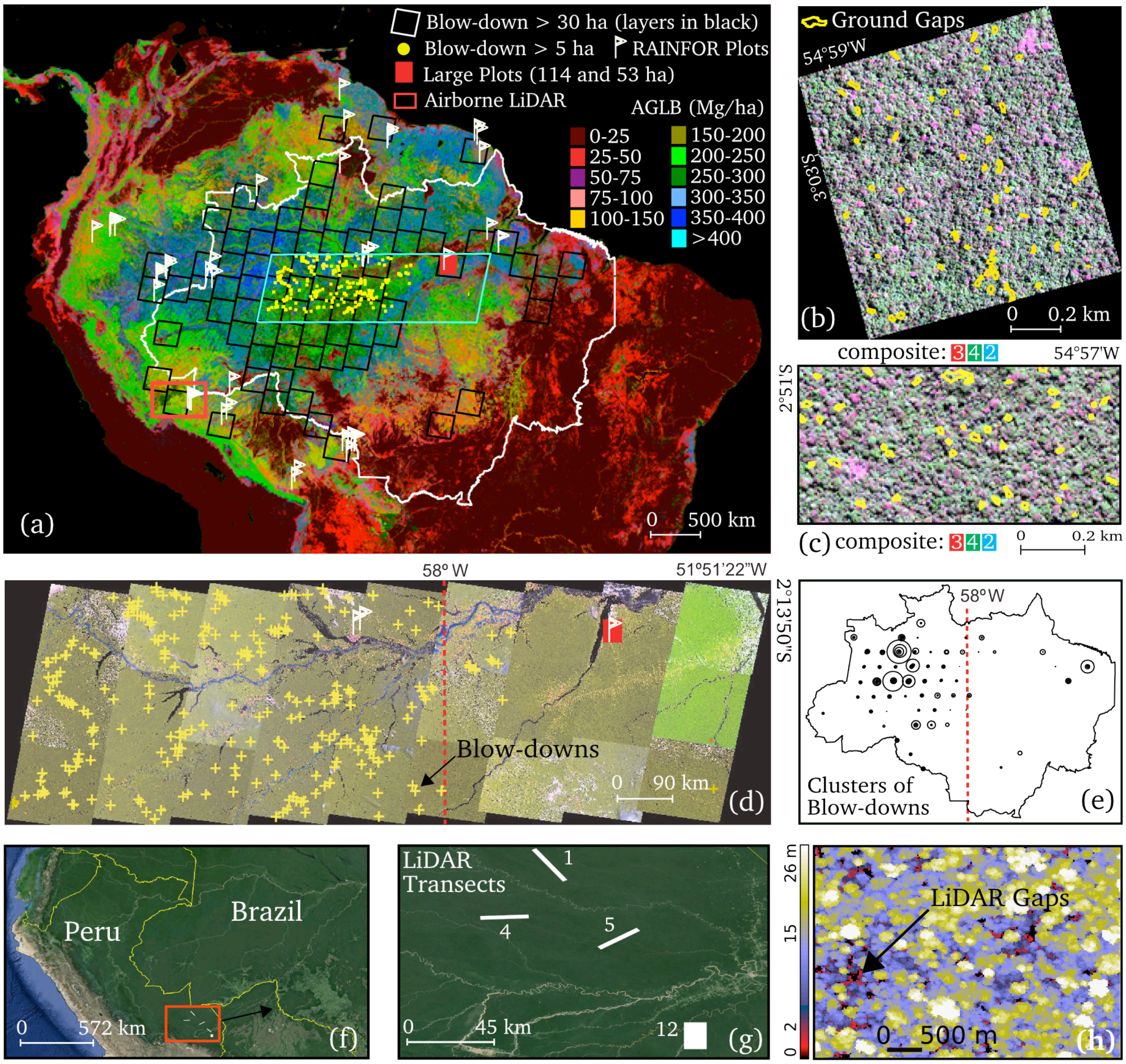

Blow-down > 30 ha (layers in black)
Blow-down > 5 ha
RAINFOR Plots
Large Plots (114 and 53 ha)
Airborne LiDAR
AGLB (Mg/ha)
0-25
25-50
50-75
75-100
100-150
150-200
200-250
250-300
300-350
350-400
>400
0 500 km
(a)
Ground Gaps
54°59'W
3°03'S
0 0.2 km
(b)
composite: 342
54°57'W
2°51'S
(c) composite: 342
0 0.2 km
58° W
51°51'22"W
2°13'50"S
Blow-downs
0 90 km
(d)
58°W
Clusters of
Blow-downs
(e)
Peru
Brazil
0 572 km
(f)
LiDAR
Transects
1
4
5
0 45 km
12
(g)
26 m
15
2
0
LiDAR Gaps
0 500 m
(h)

Figure 2

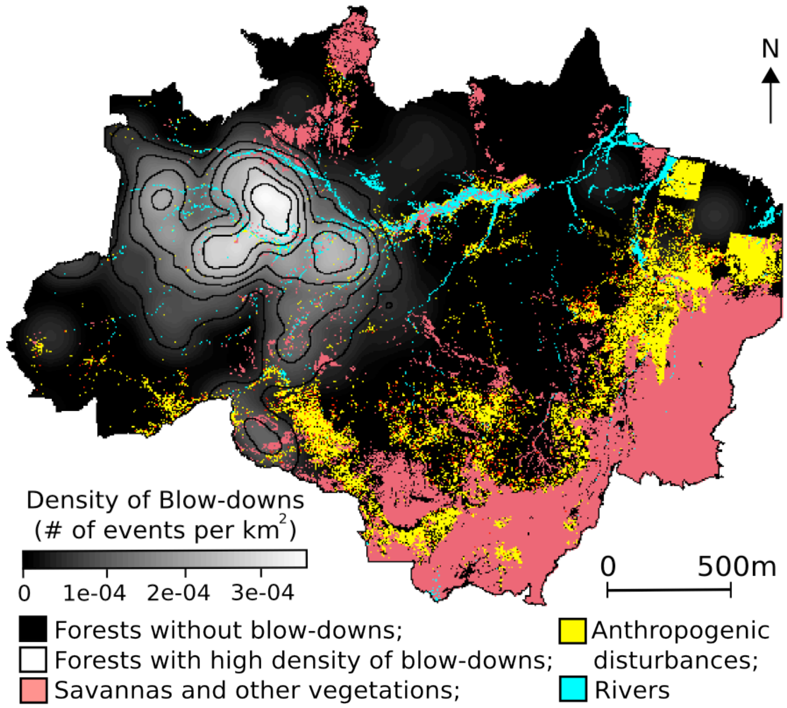
N
Density of Blow-downs
(# of events per km^2)
0
1e-04
2e-04
3e-04
0
500m
Forests without blow-downs;
Forests with high density of blow-downs;
Savannas and other vegetations;
Anthropogenic
disturbances;
Rivers

Figure 3

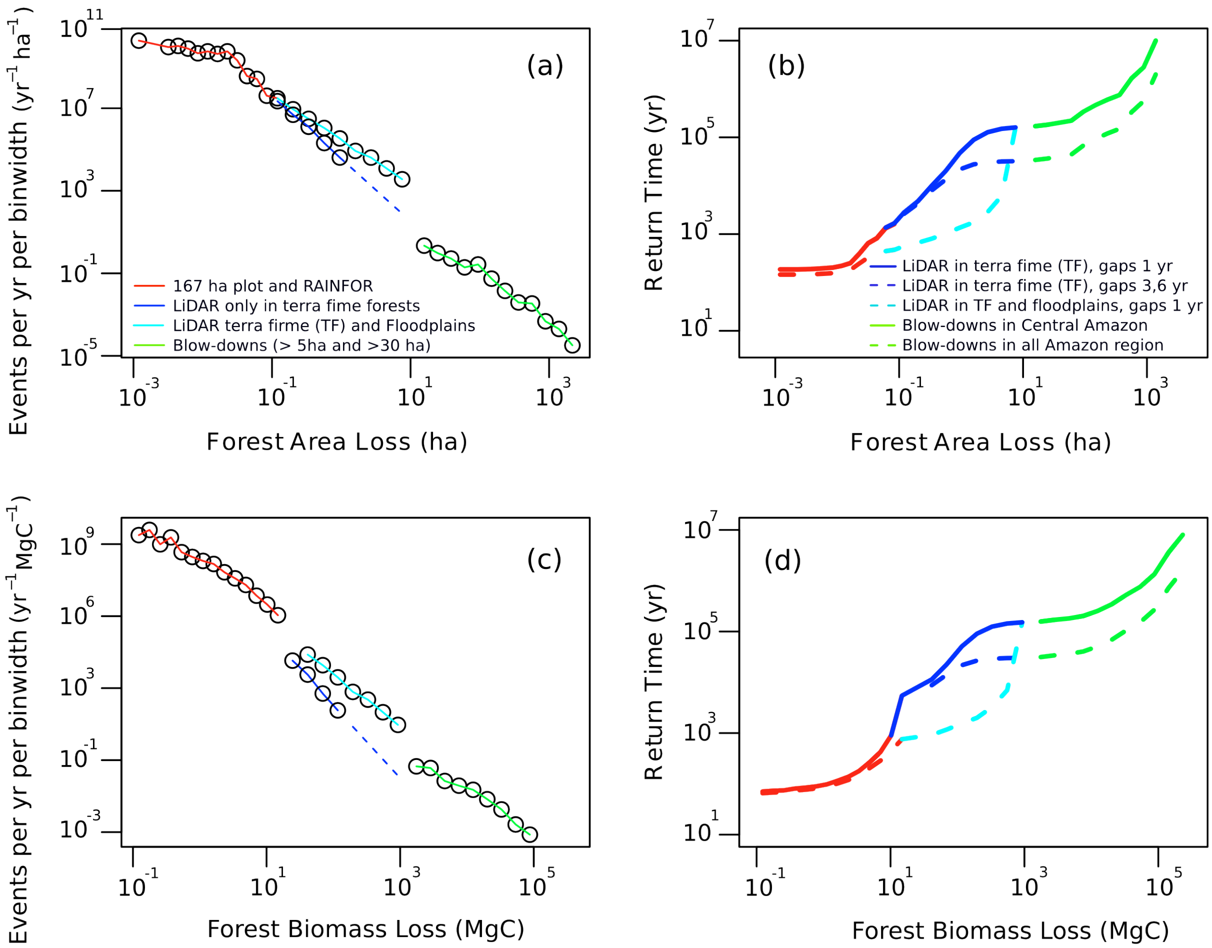
(a)
Events per yr per binwidth (yr^{-1} ha^{-1})
Forest Area Loss (ha)
167 ha plot and RAINFOR
LiDAR only in terra fime forests
LiDAR terra firme (TF) and Floodplains
Blow-downs (> 5ha and >30 ha)
(b)
Return Time (yr)
Forest Area Loss (ha)
LiDAR in terra fime (TF), gaps 1 yr
LiDAR in terra fime (TF), gaps 3,6 yr
LiDAR in TF and floodplains, gaps 1 yr
Blow-downs in Central Amazon
Blow-downs in all Amazon region
(c)
Events per yr per binwidth (yr^{-1} MgC^{-1})
Forest Biomass Loss (MgC)
(d)
Return Time (yr)
Forest Biomass Loss (MgC)

Size and Frequency of Natural Forest Disturbances and the Amazon Forest Carbon Balance

Supplementary Material

Fernando D. B. Espírito-Santo[1,2,*], Manuel Gloor[3], Michael Keller[2,4,5], Yadvinder Malhi[6], Sassan Saatchi[1], Bruce Nelson[7], Raimundo C. Oliveira Junior[8], Cleuton Pereira[9], Jon Lloyd[3,10], Steve Frolking[2], Michael Palace[2], Yosio E. Shimabukuro[11], Valdete Duarte[11], Abel Monteagudo Mendoza[12], Gabriela López-González[3], Tim R. Baker[3], Ted R. Feldpausch[3], Roel J.W. Brienen[3], Gregory P. Asner[13], Doreen Boyd[14] and Oliver L. Phillips[3]

[1]*NASA Jet Propulsion Laboratory, California Institute of Technology, Pasadena, CA 91109, USA*
[2]*Inst. for the Study of Earth, Oceans and Space, Univ. of New Hampshire, Durham, NH 03824, USA*
[3]*School of Geography, University of Leeds, Leeds, LS2 9JT, UK*
[4]*USDA Forest Service, International Institute of Tropical Forestry, San Juan, Puerto Rico*
[5]*Embrapa Monitoramento por Satélite, Campinas, SP, CEP 13070-115, Brazil*
[6]*School of Geography and the Environment, University of Oxford, Oxford, UK*
[7] *National Institute for Research in Amazonia (INPA), C.P. 478, Manaus, Amazonas 69011-970, Brazil*
[8]*Empresa Amazônia Oriental (CPATU), Santarém, PA, CEP 68035-110 C.P. 261, Brazil*
[9]*Belterra, PA, CEP 68143-000, Brazil*
[10]*Centre for Tropical Environmental and Sustainability Science (TESS) and School of Earth and Environmental Sciences, James Cook University, Cairns, Queensland 4878, Australia*
[11]*National Institute for Space Research (INPE), São José dos Campos, SP, CEP 12227-010, Brazil*
[12]*Jardin Botanico de Missouri, Oxapampa, Pasco, Peru*
[13]*Department of Global Ecology, Carnegie Institution for Science, Stanford, CA 94305, USA*
[14]*School of Geography, University of Nottingham, University Park, Nottingham, NG7 2RD, UK*

Sep 26, 2013

*Author for Correspondence:

Fernando D.B. Espírito-Santo
NASA Jet Propulsion Laboratory
California Institute of Technology
Radar Science and Engineering Section
4800 Oak Grove Drive, MS 300-319
Pasadena, CA 91109

E-mail: f.delbon@gmail.com

1. Amazon natural disturbance data We quantified the frequency distribution of small[1–4] and large disturbances[5–8] from several sources of data. Our data ranges from permanent tree plots[9–13] to satellite[5,6] or airborne LiDAR[14] images (Supplementary Tab. S1). We quantify not only data of disturbance area, but also the aboveground biomass loss in Mg C associated with these events.

Table S1. *Statistical summary of all data sets used to estimate the full frequency spectrum of disturbance over the Amazon.* 484 censuses of 135 ~1ha plots distributed over the Amazon[9–12], 48,374 ha tropical forest sampled in Southern of Peru by airborne LiDAR[14], 96 tree-fall gaps of 167 ha plot in East central Amazon[13], 279 blow-downs ≥ 5 ha detected in 27 Landsat scenes[6] and 330 large disturbances ≥ 30 ha inspected in 137 Landsat images[5]. Minus sign denotes mass losses for biomass losses.

Statistic summary	RAINFOR (484 censuses)	167 ha plot	Airborne LiDAR	Blow-downs in 27 images	Blow-downs in 136 images
Disturbances Class Size	Small	Small	Intermediate	Large	Large
Raw data for modeling	484	96	30,130	279	330
Min. disturbance area (ha)	**0.0003**	**0.003**	**0.002**	**5**	**30**
Max disturbance area (ha)	**0.09**	**0.13**	**9.48**	**2,223**	**2,651**
Mean disturbance area (ha)	0.016	0.026	0.009	79	213
Median disturbance area (ha)	0.013	0.022	0.003	37	123
SD of disturbance area (ha)	0.012	0.018	0.079	179	279
Sum of disturbance area (ha)	7.53	2.51	294.50	21,931	70,421
Min. biomass loss (Mg C)	**-0.055**	**-0.061**	**-0.1**	**-324.9**	**-3,068**
Max biomass loss (Mg C)	**-11.69**	**-19.90**	**-1,162**	**-389,131**	**-463,876**
Mean biomass loss (Mg C)	-2.32	-3.05	-1.04	-12,091	-30,198
Median biomass loss (Mg C)	-1.99	-1.63	-0.29	-5,239	-17,672
SD of biomass loss (Mg C)	-1.61	-3.61	-9.75	-31,347	-42,893
Sum of biomass loss (Mg C)	-1,126	-293.67	-31,474	-3,373,601	-9,965,230

1.1. Data integration A flowchart summarizes all processing steps used to harmonize the data of natural disturbances over the entire Amazon region (Supplementary Fig. S1). Five data sources were used to estimate disturbances: at small-scale (1) data set from two large plots[13] (167 ha) in Tapajós region, and (2) 484 repeat censuses of the tropical forest network[9,11,12,15]; at intermediate: (3) LiDAR from Southern Peruvian Amazon[14] (48,374 ha); and at large-scale: (4) blow-downs > 30 ha (n=330) covering the entire Brazilian Amazon, and (5) fine resolution blow-downs > 5 ha (n=279) covering a East-West Amazon forest region transect. Because each data source was collected and produced in different ways, we applied several intermediate steeps to estimate and normalize the data. Our final goal was to use the probability distribution of (*i*) area and (*ii*) biomass loss of natural disturbances to understand the trajectory of the Amazon forest carbon balance.

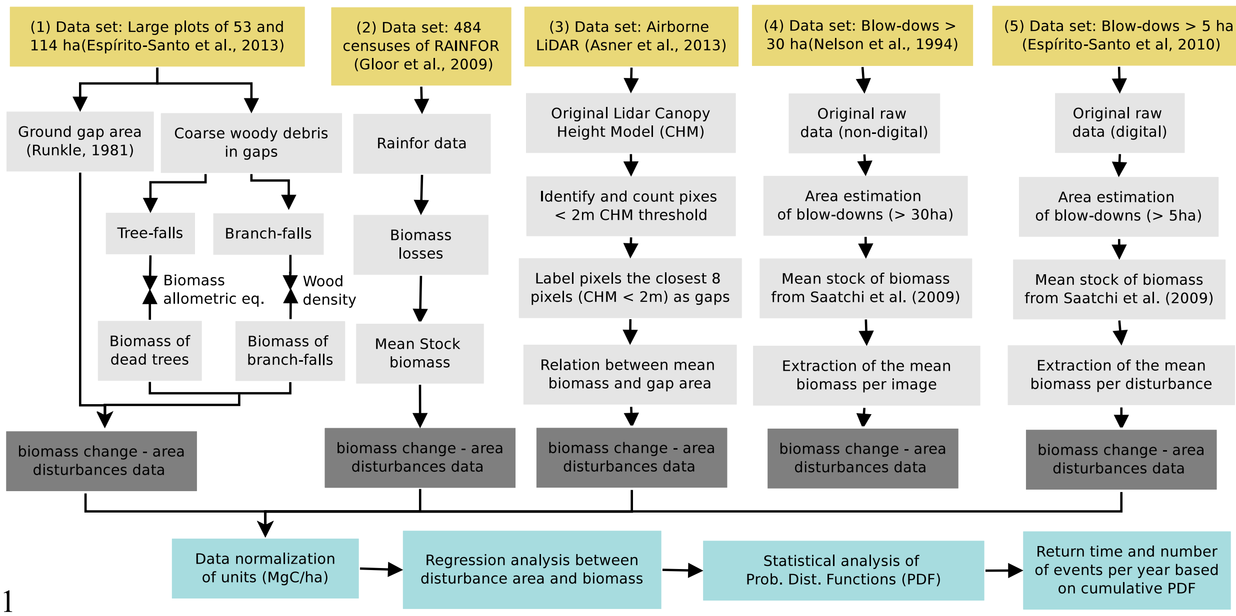

Supplementary Figure S1. *Schematic outline.* Main processing steps carried out to integrate several sources of disturbance data over the Amazon region.

2. RAINFOR plots We used the extensive historical data set of the RAINFOR plots[9–12,15–18] based on net changes in biomass (Mg C ha^{-1} yr^{-1}) which include two aboveground biomass flux terms[19,20]: biomass gains (from tree growth and recruitment) and biomass losses (from tree mortality). The biomass losses from these plots were assessed to provide information of tree mortality across the Amazon region. Those plots are typically 1 ha in size and measurement details have been described elsewhere[9,11,12,17,18]. The available, published RAINFOR data (135 plots[12]) cover a total area of 226.2 ha with a mean total monitoring period of 11.3 years. Aboveground biomass was estimated from tree diameter and wood density (based on species identity) by allometric equations[21]. Mortality rates have been corrected for census-interval effects[22].

2.1. Translating biomass loss measured in RAINFOR plots to disturbance area The RAINFOR network does not record data for disturbance area - only biomass losses by mortality events – so we estimated the area of those disturbances associated with the biomass loss as gap area of a given plot = {plot mortality or mean biomass loss (ha^{-1})} ÷ {total stock of biomass (ha^{-1})}. We caution that this approach assumes that all biomass disturbances are linearly correlated with area of the disturbances which is a rough approximation[23]. Moreover, ground data of tree-fall gap disturbance areas and biomass losses from two large plots in Tapajós National Forest (54 and 114 ha, n=96 gaps) suggests that this relation is not linear (Supplementary Fig. S3). However, although not universal, we used your allometric equation of biomass losses based on disturbance areas to assess the mean losses of biomass over a several landscape-scale areas of Amazon.

3. Large forest inventory plots data RAINFOR data[9] do not account for biomass losses (disturbances) that do not result in complete tree mortality (e.g. coarse woody debris (CWD) produced by partial crown-falls). To evaluate carbon losses including both complete and partial mortality, we installed and surveyed two large forest inventory plots[13] of 114 and 53 ha, in unmanaged forest area in the eastern central Amazon, Tapajós National Forest (TNF) (Fig. 1 and Supplementary Fig. S3). The first plot was installed in 2008 and the second in 2009. The methodology to assess the biomass losses (CWD) inside of the gaps areas has been described elsewhere[13], with the main steps listed here:

1) We mapped all gaps in both large plots using the Runkle gap definition[24];

2) We defined the modes of gap-formation[1–4,24] based on the type of disturbance (partial or complete crown-fall, snapped bole-fall, and uprooted tree-fall);

3) We classified all gaps within two age classes (< 1 and ≥ 1 year old);

4) We measured the volume of all CWD for each gap identified in the field;

5) We used an allometric equation[25] to estimate woody biomass losses by fresh tree–falls and snapped bole falls while for gaps with partial crown-fall we recorded the diameters of all wood pieces greater than 10 cm and length of the woody material;

6) We classified the decomposition status[26–28] of all CWD into five decay classes - from freshest (class 1) to most rotten (class 5) material;

7) We used an average of CWD density measured for each decay class specifically developed for this site[27–29];

8) We calculated the sectional volume of each segment of CWD; and

9) We estimated the mass of CWD from the product of the volume of material and the respective density for the material class[27–29].

3.1. Biomass losses measured at the large forest inventory plots In the two large plots[13] (167 ha total area) we found 96 gaps. In TNF the mean tree mortality was 2.38 stems ha^{-1} $year^{-1}$. CWD amounts depended on the type of gap formation, crown-falls contained 0.11 Mg C ha^{-1} of CWD, snapped tree-falls 0.65 Mg C ha^{-1} and uprooted tree-falls 0.70 Mg C ha^{-1}. The flux of CWD caused by the gaps was 0.76 Mg C ha^{-1} $year^{-1}$. The average mortality of trees (DBH ≥ 10 cm) per gap was 6.5, resulting in a total of 596 dead individual trees (3.57 trees ha^{-1}; > 10 cm DBH) for the total surveyed area of 167 ha. From the total dead trees contained in the gaps of all ages, we estimated a mean annual tree mortality of 2.38 trees ha^{-1} $year^{-1}$.

4. Airborne LiDAR data To estimate the distribution of intermediate scale sized disturbances[30,31] (between 0.01 and 5 ha of opened area) we used a large collection of airborne LiDAR[14] images. LiDAR (Light Detection and Ranging) is a remote sensing technology that measures distances by illuminating a target with a laser and analyzing the reflected light[32]. Recently, airborne LiDAR has been used to distinguish canopy gaps at large spatial scales[14,33,34], providing a unique opportunity to understand the frequency distribution of natural disturbances or tree-fall gaps.

We used LiDAR data collected by the Carnegie Airborne Observatory (CAO) Alpha System[35] (July 2009) in the Southern Peruvian Amazon[14]. The study was undertaken in the Madre de Dios watershed, in a region of well-known geologic and topographic variation in lowland forest close to the base of the Andes in Peru[14]. Briefly, the flights were conducted at 2000 m aboveground level at a speed of <95 knots. The LiDAR was operated with a 38-degree field of view and 50 kHz pulse repetition frequency, resulting in 1.1 m laser spot spacing[14]. We processed 4 blocks (Fig. 1g) covering a total of 48,374 ha. To compare gap-size frequency distributions among forests in the lowland Peruvian

Amazon, LiDAR data was classified in each block by its geologic composition and an empirical LiDAR digital terrain model of ~15 m tree height[14], resulting in two major types of forest areas[14]: “depositional-floodplain” (DFP) in 15,178 ha and erosional “terra firme” (ETF) in 33,196 ha (following the abbreviations in Asner et al[14]). Terra firme forests dominate Amazonia (RAINFOR[9,10,12,18,36]), we used the DFP data only for a sensitivity analysis of our forest simulator results to different forms of the Amazon disturbance frequency distribution.

To quantify all types of natural disturbances at landscape scale with LiDAR (i.e. from small 0.01 ha to intermediate scales 5 ha), the original LiDAR laser data points were processed[14] to generate raster images (pixel resolution = 1 m) of the digital canopy surface model (DSM) and digital terrain model (DTM). The DSM was based on interpolations of all first return points of the cloud data, where elevation is relative to a reference ellipsoid. The DTM was based on a 30 m x 30 m filter passed over each flight block and the lowest elevation estimate in each kernel was assumed to be the ground. Canopy heights (DCM) were estimated as the difference between the canopy surface model and the digital terrain model, i.e. as DCM=DSM-DTM[14] (Supplementary Fig. S2).

Because LiDAR data analyses permit detection of all gaps extending from the top of the canopy to different heights aboveground[14,33,34] (i.e. 1-2 m tree height), we defined gaps in our LiDAR data using the ecological definition of Brokaw[2]: gaps in LiDAR digital canopy model are openings in the forest canopy extending down to an average height 2 m aboveground (Supplementary Fig. S2c,d). The minimum gap size considered was 20 m^2 (Supplementary Fig. S2e).

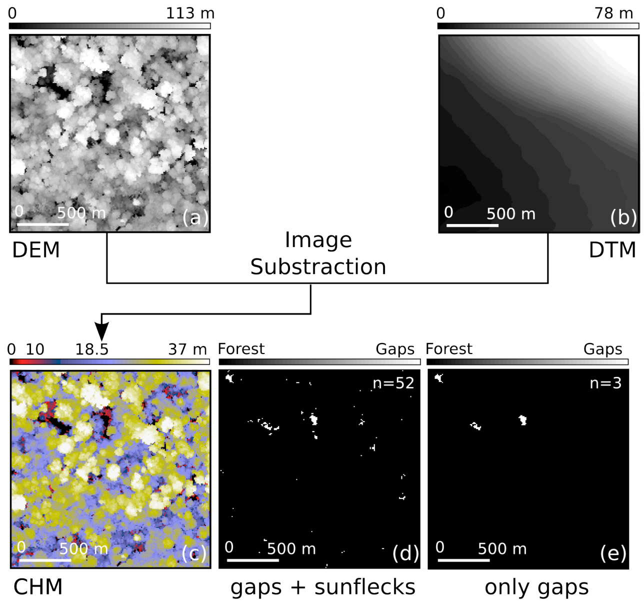

Supplementary Figure S2. *Example of image processing to extract and detect tree-fall gaps in LiDAR images.* Digital canopy surface model (a) and digital terrain model (b) were extracted from LiDAR cloud laser points to produce the digital canopy model or tree height (c). Forest sunflecks[37] (in this case 52 in number) detected by LiDAR (d) were separated from tree-fall gaps (in this case 3) using a minimum gap-size threshold of 20 m^2 (e). LiDAR grid image of 200 m by 200 m (4 ha).

<u>4.1. Biomass loss associated with intermediate-scale disturbances</u> To estimate biomass loss due to intermediate-size disturbance detected by LiDAR images (4 transects with a total of 48,343 ha, n=30,130 gaps) we used an allometric equation of biomass loss (Mg C) based on gap size of disturbances (ha) collected on the ground in two large forest inventories[13] (Supplemental Fig. S3). We used a minimum gap size area threshold of 20 m^2 of disturbance area to estimate CWD or biomass loss inside of tree-fall gaps areas detected by LiDAR. There are two reasons for using this approach: (1) based on our previous analysis, measurable carbon loss was associated with a minimum gap area of ~20 m^2 or bigger (see Espírito-Santo et al., 2013[13]) whereas (2) very small gaps (i.e. ~1 m^2) - where most of the sunflecks[37] occur - are probably more related with tree crown spacing[37] than with biomass carbon dynamics.

We estimated the necromass of small-intermediate disturbance areas detected by LiDAR[14] using a linear regression model of aboveground biomass loss (Mg C) as a function of gap-size area (ha) of central Amazon[13] (167 ha plot, n=96) (Supplemental Fig. S3). The resulting equation to estimate necromass from tree-fall gaps[13] does not represent all of the Amazon and may slightly overestimate carbon loss in Peru where wood density tends to be lower than in the Central Amazon[23].

Finally, the LiDAR datasets available currently are not repeat surveys so only permit a snapshot of forest structure to be taken. To use these data to inform forest biomass dynamics evidently requires making a number of important assumptions about how these maps of gaps translate into forest disturbance rates. To ensure that our test of the hypothesis that the plot network effectively measures biomass change is conservative, our assumptions deliberately err on the generous side to the magnitude and frequency of intermediate area disturbance. Our assumptions will tend to overestimate the rate of formation of intermediate-sized gaps, and therefore should overestimate their contribution to Amazon biomass dynamics. Notably, we assume

(1) That the region surveyed is representative of Amazonia. In fact we know from our ground work that forests in western Amazonia have much faster biomass turnover and a greater proportion of tree death caused by exogenous disturbance than elsewhere (e.g., Phillips et al. 2004, Galbraith et al. 2013)[38,39].

(2) That gap recovery rates are fast, with 50% closure within 3.6 years. This estimate is based on a transition matrix from Hubbell and Foster (1986)[40], indicating that at Barro Colorado Island, Panama, the 1-year transition probability for 5*5m gaps to non-gaps was 0.177. Alternatively, a study from French Guiana suggests a half-life of between 5 and 6 years (Fig 7 in Van de Meer and Bongers, 1996[41]), and with all gaps closing after about 15 years.

(3) That gap recovery rates are independent of size within the 'intermediate' part of the spectrum. In practice, bigger gaps will take longer than small gaps to close so our approach is likely to overestimate the frequency of larger gap formation

(4) Our estimated gap formation rates are translated into biomass dynamics estimates assuming an AGB value of 170 Mg C ha^{-1}. In fact, in 16 * one-hectare plots in the same region where the LiDAR imagery were taken, mean AGB is 119 Mg C ha^{-1}. This assumption alone therefore results in overestimating the impact of intermediate biomass disturbances in south-western Amazonia by more than 40%.

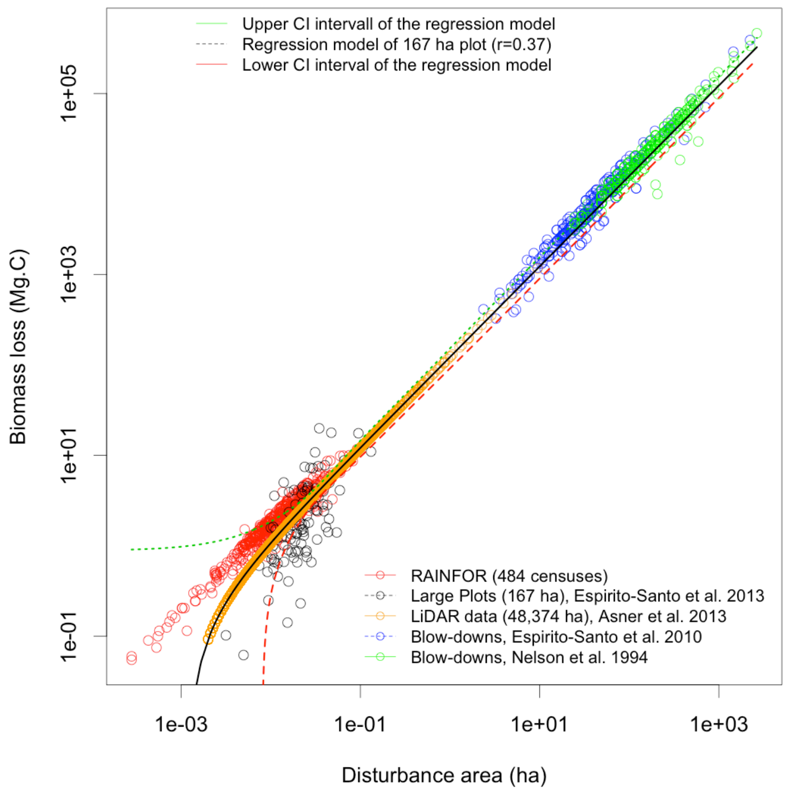

Supplementary Figure S3. *Relation between disturbance area and loss in aboveground biomass in the Amazon.* Data sets are from several studies of disturbances across the Amazon, from branch and tree falls to landscape scale blow-downs. Small disturbances: (1) in red, forest plot inventories (n=484 censuses of 135 * 1ha plots[12]) distributed over the Amazon and (2) in black, 96 tree-fall gaps from two large forest inventory plots (total area 167 ha) in the Tapajós National Forest[13]. Intermediate disturbances: (3) in orange, small and intermediate disturbances from 48,374 ha of LiDAR[14] images. Large disturbances: (4) in blue, 279 blow-downs bigger than 5 ha from an East-West mosaic of 27 Landsat scenes of the Amazon[5]; and (5) in green, 330 blow-downs greater than 30 ha from 136 Landsat scenes in the Brazilian Amazon[6]. A relation between area and biomass loss (Mg C) was tested from 96 tree-fall gaps (0.003 - 0.13 ha) where both area and aboveground biomass were measured. The linear regression fit is Biomass Loss = -0.1528 + 122.5073 (Disturbance Area) (n=96, r=0.37), in units of Mg C and ha for loss biomass and disturbance area, respectively.

5. Amazon intact forest area To scale up our results of natural forest disturbances from forest inventory plots[9,12,13], LiDAR[14] and satellite images[5,6], to the entire intact forest area of the Amazon, we used a land cover map with 250 m spatial resolution for all countries that are part of the Amazon tropical forest biome[42] (Supplemental Fig. S4). For the Brazilian Amazon region (approximately 60% of the entire Amazon) we used the land use map from the annual deforestation monitoring project (PRODES) of the National Institute for Space Research (INPE)[42] to separate old-growth forest from non-forest areas or recently deforested areas. PRODES has monitored tropical deforestation in Brazil over the last 30 years using historical Landsat images[43] using visual interpretation and digital image processing[44]. To expand the land use map to South America (Pan-Amazon Project, unpublished data[42]), multi-temporal MODIS images of 250 m resolution were processed by the INPE Pan Amazon project[42] for the others regions and integrated to the PRODES database[43]. The land use map (Supplementary Fig. S4) has the following categories: undisturbed forest, deforestation (general category of bare soils, secondary forests and burned areas), and other types of vegetation (savannas and grasses). According to this map the total area of undisturbed forest in northern South America is 6.8×10^6 km^2 covering the Amazon drainage region and the contiguous Andes and Guyana's regions[45] - the entire forested Brazilian Amazon is 3.5×10^6 km^2.

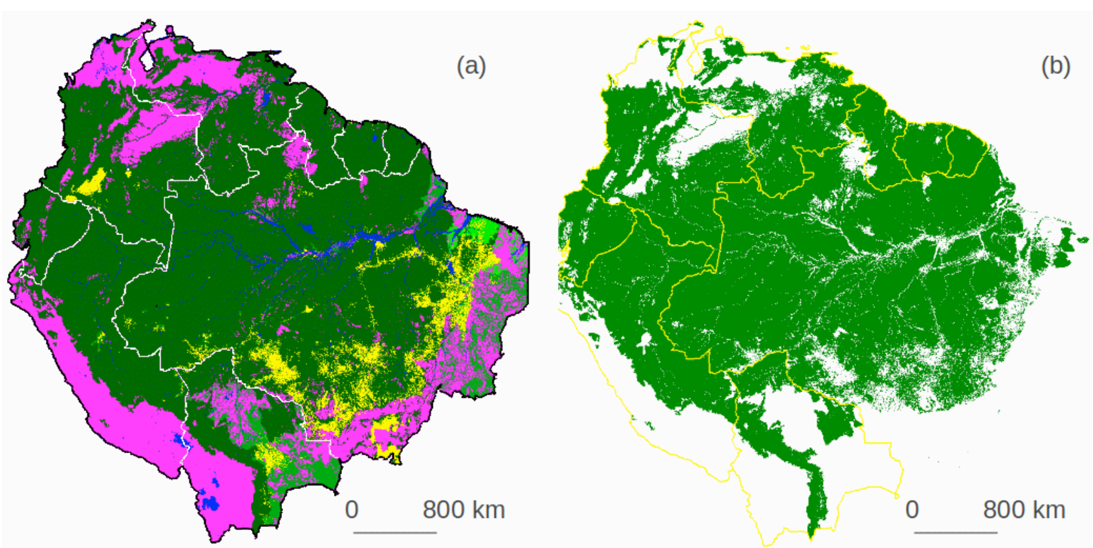

Supplementary Figure S4. *Amazonia land cover map.* Map using historical Landsat and MODIS images (a) from the Pan-Amazon project for the year 2010. Undisturbed forests of tropical regions (b), excluding other types of land cover. Map colors represent the following categories: undisturbed forest (dark green), deforestation (yellow), savannas or/and grass vegetation (pink), secondary forest (light green) and water (blue).

We used the entire Amazon region (6.8 x 10^6 km^2) to scale up all natural disturbances (Supplementary Tab. S1) recorded in our data. Considering that most of the blow-downs are concentrated in Central Amazon, we assumed that large disturbances cover 1/5 of the total area of our entire domain of Amazon forests (see also Tab. 1 for more details).

6. Basin-wide large disturbance data We developed a spatially explicit analysis of large disturbances (blow-downs) in the Brazilian Amazon tropical forest biome based on extensive samples of Landsat satellite images (30 m). We assessed the occurrence and spatial distribution of 330 events of large disturbances or blow-downs (≥ 30 ha) during the period from 1986 to 1989 based on 137 Landsat images[46,47] (Supplementary Fig. S5) using the original raw data from the first study that described the occurrence of blow-downs in the Amazon[5].

We also analyzed the occurrence and spatial distribution of 278 large forest disturbances (≥ 5 ha) from 1999 to 2001 apparently caused by severe storms in a mostly unmanaged portion of the Brazilian Amazon using 27 Landsat images and digital image processing[6].

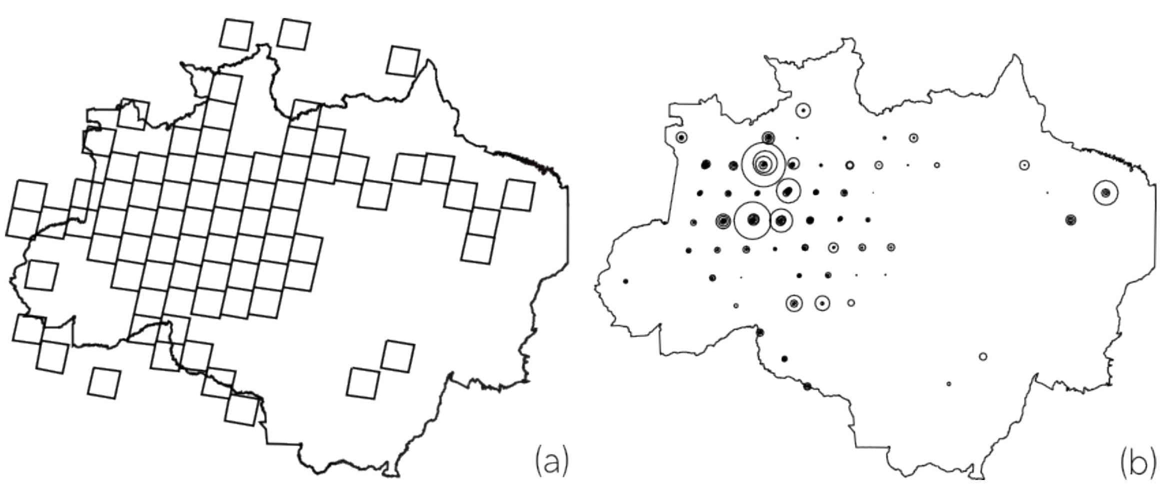

Supplementary Figure S5. *Landsat images and blow-down distribution.* Spatial distribution of 72 Landsat scenes with the occurrence of blow-downs from the total 136 surveyed scenes of the Brazilian Amazon[5] (a). The area of blow-down disturbance is proportional to the size of the circles (b). Landsat images with blow-downs outside of the Brazilian Amazon border were omitted from the spatial point analysis.

6.1. Spatial distribution of large disturbances Previous analyses of large disturbances showed that blow-downs are extremely rare in Eastern Amazonia[5,6]. To account for clustering of large disturbances in the Amazon we reanalyzed the original data of large natural disturbances from Brazil[5] using a spatial point analysis (SPA)[6]. A SPA consists of a set of points (s_1, s_2, …, s_N) in a defined study region (R) divided into sub-regions ($A \subseteq R$). $Y(A)$ is the number of events in sub-region A. In a spatial context, the number of points can be estimated by use of their expected value $E(Y(A))$, and covariance COV ($Y(A_i)$, $Y(A_j)$), given that Y is the event number in areas A_i and A_j. The intensity of an event $\lambda(s)$ is the frequency per area of points of a specific location s, where ds is the area of this region, i.e. $\lambda(s) = \lim_{ds \to 0} \left\{ \frac{E(Y(ds))}{ds} \right\}$. Because SPA only requires the spatial location of each event, we used the center of each classified blow-down in the Landsat images. We used a Gaussian algorithm (kernel smoothing) with bandwidths between 100 and 250 km to calculate the smooth intensity field from our data. The minimum mean square error (MSE) of the Gaussian kernel smoothing algorithm[46,47] revealed that the bandwidths ~ 200 km (Supplementary Fig. S6) is the most indicated to estimate the intensity of blow-downs in the Amazon. The probability density function k of Ripley[46] also suggests that large-scale disturbance blow-downs in the Amazon are strongly clustered[6] for the tested bandwidths (Supplementary Fig. S7).

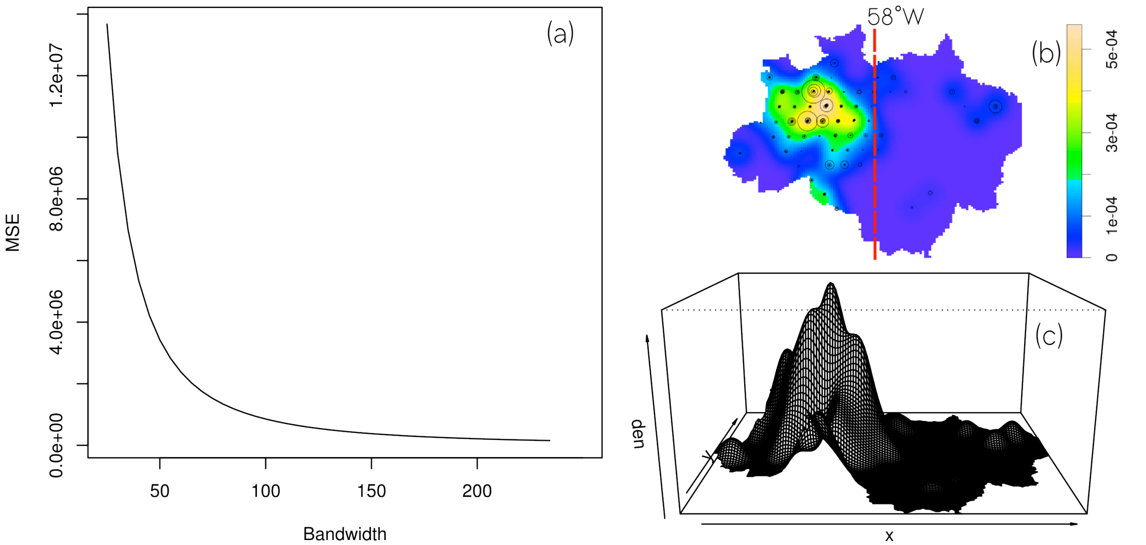

Supplementary Figure S6. *Kernel bandwidth distribution.* Mean square error (MSE) of the Gaussian kernel smoothing algorithm[46,47] (a) from the spatial distribution of 330 blow-downs data[5]. The bandwidth with smaller MSE around 200 km (b) is the less biased bandwidth for this spatial data. East-West perspective graph of the intensity of blow-downs in the Amazon (c) produced by a smoothing kernel interpolation.

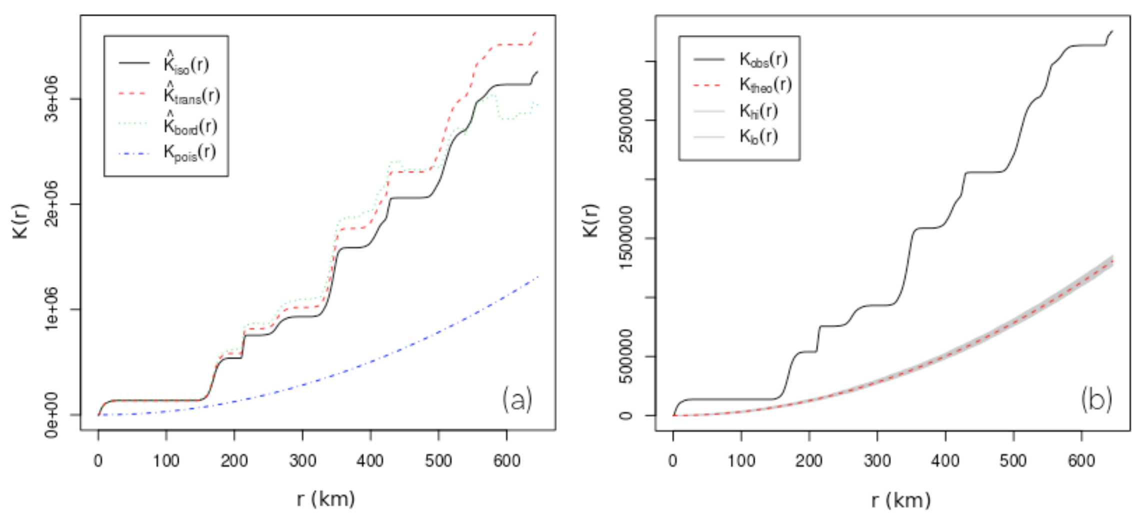

Supplementary Figure S7. *K-function distribution of the spatial patterns of blow-downs. K*-function (a) and simulated envelops of the spatial distribution of 330 blow-downs[5] (a). Monte Carlo simulation (*T*=1000) of the *K*-function[46] (b). Color lines in *a* are the theoretical Poisson *K(pois)* of *K*-function in blue and the border-corrected estimate *K(bord)* in green, translational-corrected estimate *K(trans)* in red and the original Ripley isotropic correction *K(iso)* in black. Color lines in *b* are the original *K*-function[46] in black and red dash lines with upper and lower envelops in grey. Graph suggests that for all spatial simulations[47] the occurrences of blow-downs are clustered significantly.

To determine the spatial distribution of blow-down over the entire region of Brazilian Amazon excluding the regions of intense land-use activities[48,49] (i.e. deforestation and fire) and other types of vegetation (i.e. savannas and sand forests) we used a land-use map (Pan-Amazon Project, unpublished data[42]) as described before. We excluded most of the anthropogenic disturbances caused by fires, but probably we did not remove some areas of undisturbed forests affected by the natural dynamics of fires (i.e. transitional regions of forest and savannas). Moreover, natural fires would play similar or stronger role in tree mortality than blow-downs and future efforts shall attempt to understand the scale and impact of natural fires on tree mortality in the Amazon[23].

The overlay of our most recent spatial grid of blow-downs (data from Nelson et al. 1994[5]) modeled with different kernel bandwidth[46] (100, 150, 200 and 250 km) from our SPA model confirmed that most of the large disturbances blow-downs in the Amazon are far away from the deforestation arc. Spatial patterns of clustering of blow-downs are influenced by the choice of kernel bandwidth sizes (Supplementary Fig. S8). However, the bandwidth with smaller MSE[46] (200 km, Supplementary Fig. S6) seems to be the most appropriate to resent the spatial pattern of blow-downs in the Brazilian Amazon. Yet, independent of the bandwidth choice, the analysis shows the same main spatial patterns of blow-downs. The density of large-scale blow-downs in the Amazon increases from East to West and South to North with the epicenter blow-downs around of Purus River region[5,6].

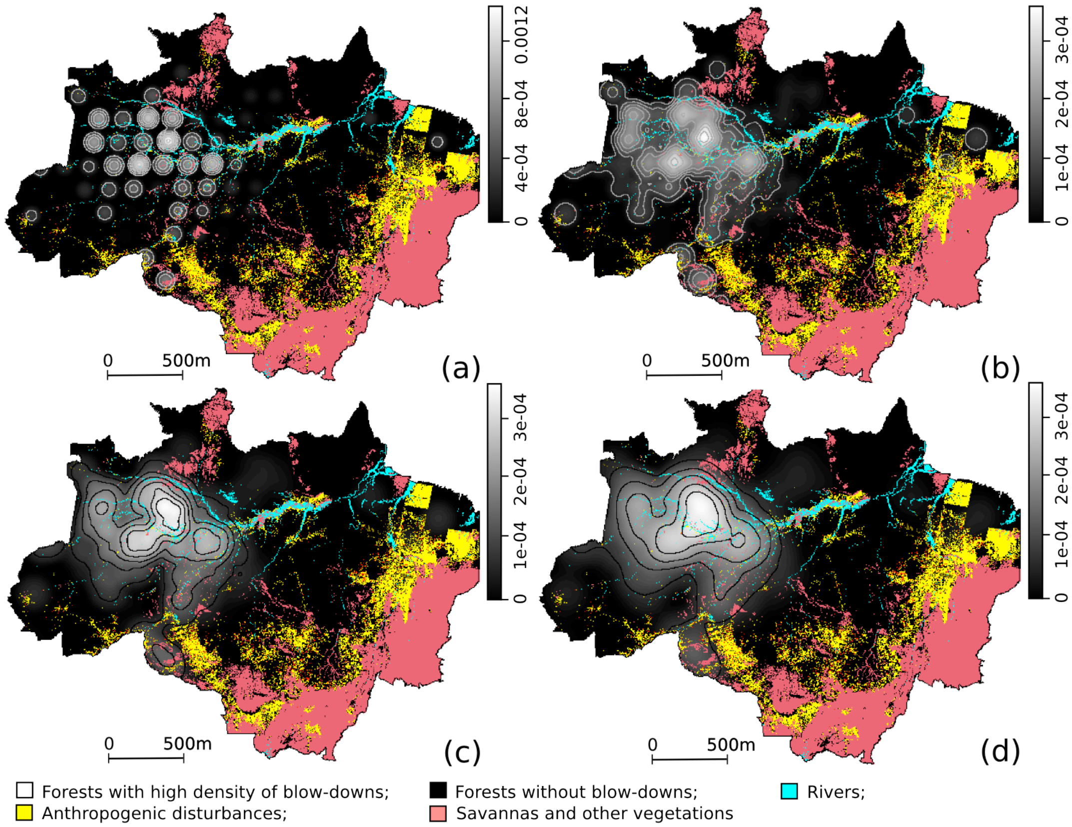

Supplementary Figure S8. *Clustering of large disturbances blow-downs in the Brazilian Amazon.* Blow-down clusters modeled with Kernel bandwidth of 100 (a), 150 (b), 200 (c) and 250 (d) km. Spatial patterns of blow-downs overlaid on a land-use and vegetation map produced by the Brazilian Space Agency INPE[42].

<u>6.2. Biomass loss of large-Scale disturbances</u> For all events of large-scale blow-downs[5,6] (n=609, sum of blow-down records of Nelson et. al, 1994[5] and Espírito-Santo et al., 2010[6]), we estimated the biomass loss as the product of disturbance area and its respective mean aboveground biomass extracted from the regional map of biomass stock of the Amazon[50] region with 1 km^2 spatial resolution (Fig. 1). We assume 100% mortality in areas of blow-downs[5,6,8,23,51]. We anticipate that this mortality rate overestimates carbon loss[23,31,52], and so provides an upper bound estimate of the significance of large natural disturbances[30,52] to old-growth forest carbon accumulation rates. Although not perfect, we provide the closest estimation of biomass loss by blow-downs based on class size of large-scale disturbances and the spatial gradient of biomass distribution in the Amazon[50].

7. Disturbance area and biomass loss From tree-fall gaps to landscape blow-downs we provide the statistics of natural disturbances data for the various data sets in terms of area and biomass loss (Supplementary Fig. S9).

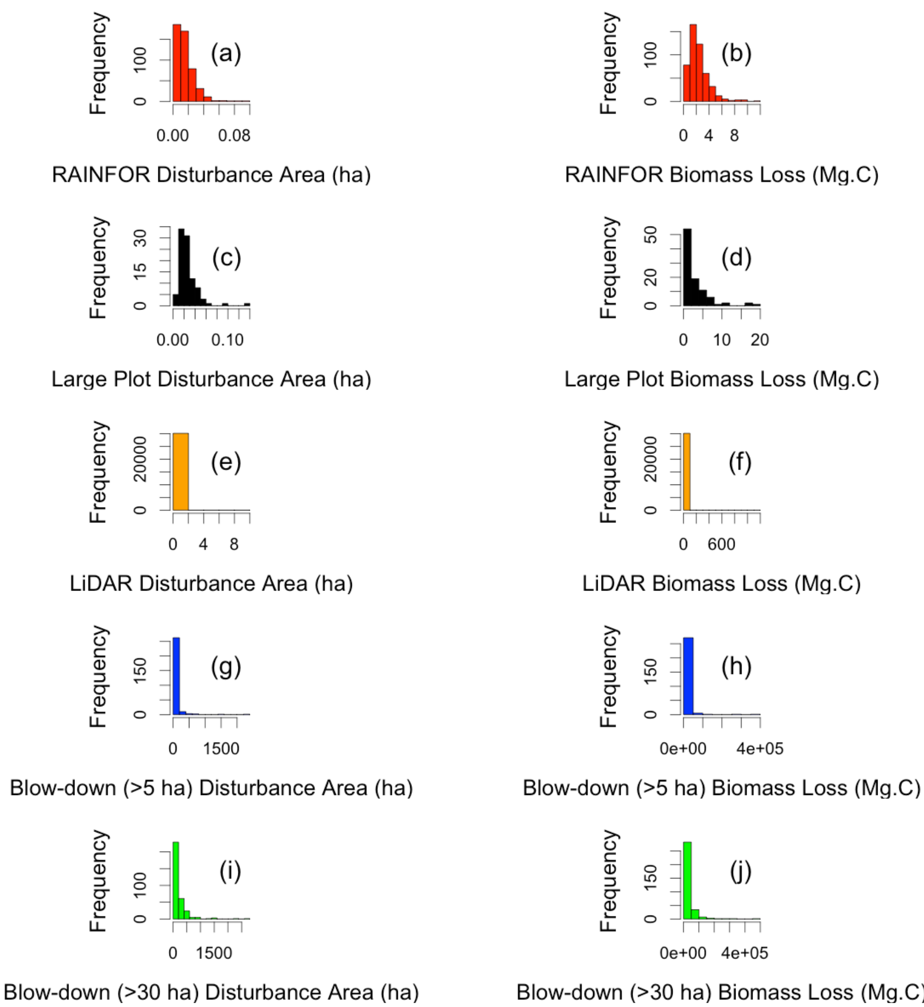

Supplementary Figure S9. *Frequency distributions of area and biomass loss from five sources of natural disturbance data sets.* Small disturbances: (1) in red, forest plot inventories (n=484 censuses of 135 * 1ha plots[12]) distributed over the Amazon (a-b) and (2) in black, 96 tree-fall gaps from two large forest inventory plots (total area 167 ha) in the Tapajós National Forest[13] (c-d). Intermediate disturbances: (3) in orange, small and intermediate disturbances from 48,374 ha of LiDAR[14] images in southern Peru (e-f). Large disturbances: (4) in blue, 279 blow-downs bigger than 5 ha from an East-West mosaic of 27 Landsat scenes of the Amazon[5] (g-h); and (5) in green, 330 blow-downs greater than 30 ha from 136 Landsat scenes in the Brazilian Amazon[6] (i-j).

Because several data have the frequency distribution concentrated over small range of the data (skewed frequency distribution), we also provide the histograms of disturbances in a log transformation for a better visualization (Supplementary Fig. S10). In general, the frequency distributions of the different types of disturbances do not overlap completely (Supplementary Fig. S10) and our data set covers all scales of natural disturbances.

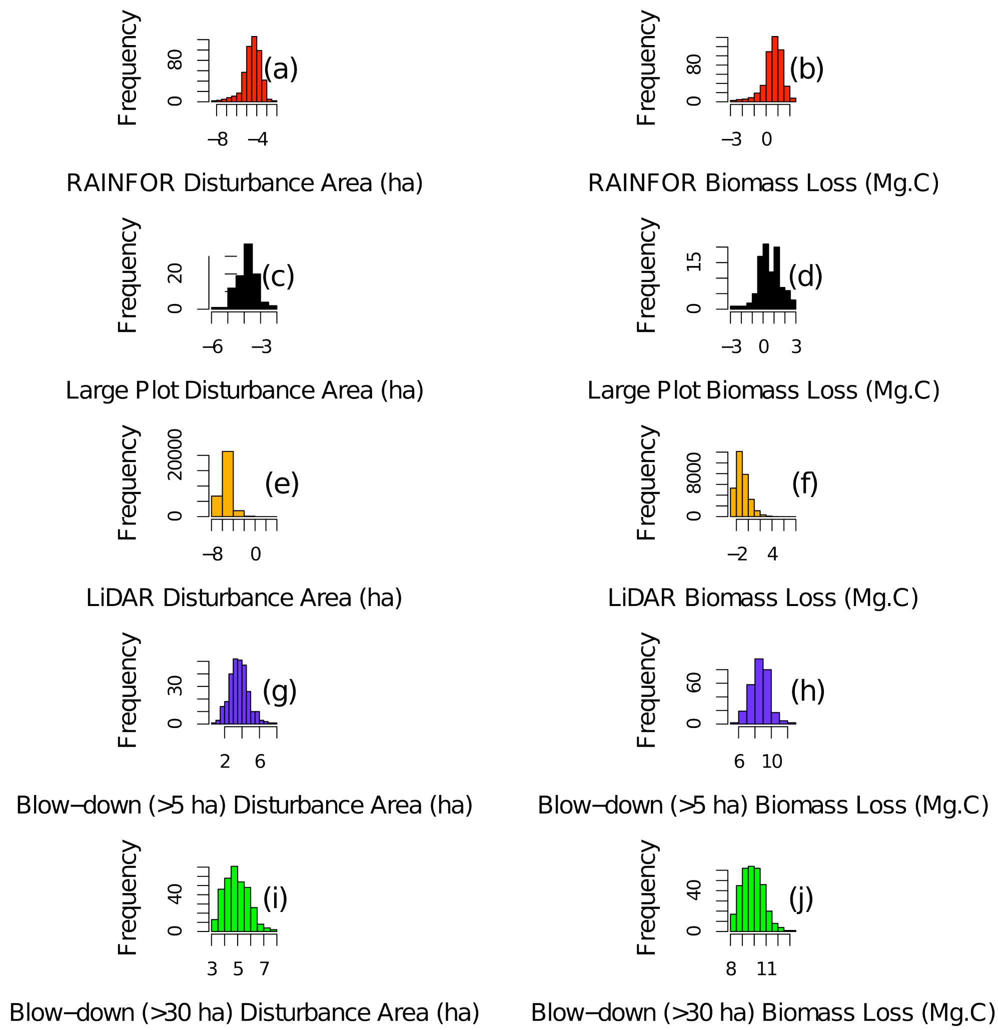

Supplementary Figure S10. *Frequency distributions (in log-scale) of area and biomass loss from five sources of natural disturbance data sets.* Small disturbances: (1) in red, forest plot inventories (n=484 censuses of 135 * 1ha plots[12]) distributed over the Amazon (a-b) and (2) in black, 96 tree-fall gaps from two large forest inventory plots (total area 167 ha) in the Tapajós National Forest[13] (c-d). Intermediate disturbances: (3) in orange, small and intermediate disturbances from 48,374 ha of LiDAR[14] images in southern Peru (e-f). Large disturbances: (4) in blue, 279 blow-downs bigger than 5 ha from an East-West mosaic of 27 Landsat scenes of the Amazon[5] (g-h); and (5) in green, 330 blow-downs greater than 30 ha from 136 Landsat scenes in the Brazilian Amazon[6] (i-j).

8. Assessing uncertainties of the natural disturbance Our general approach to quantify uncertainties is to use simulation scenarios that bracket the likely range of outcomes associated with various specific sources of uncertainty.

Uncertainties of our analysis are associated (*i*) with combining datasets to obtain a region-wide disturbance size frequency distribution and (*ii*) simulation results based on such distributions. In order to address (i), we note that the methods for detecting disturbances used in this study are suitable for different spatial scales (e.g. Landsat suitable to detect large blow-downs) and mostly do not overlap with respect to disturbance size range. If the datasets do not overlap we scaled them to the full region by multiplication with Amazon forested area-to-area probed before combining them (forests censuses, LiDAR imagery, Landsat imagery). In this case there is no need to take into account uncertainties for the combination (not for assessing uncertainties related to the simulations though – which we address as explained under the simulation Table 1). Where there is overlap in the size range covered by different datasets (relevant only to different plot data) obtained with different methods we combined the data by weighing inversely with area probed.

To address (ii) we first briefly recapitulate our data sets and their spatial coverage. For smallest disturbances monitored by forest censuses (RAINFOR data[12]) spatial coverage is very good with plots distributed well along the major axes of variation[9] (soil fertility, dry season length, El Nino influence) (Fig 1a). Largest disturbances are observed with Landsat imagery[5,6] which cover approximately 60 % of the Amazon forest region and the dataset includes 609 blow-downs (sum of blow-down records of Nelson et. al, 1994[5] and Espírito-Santo et al., 2010[6]). As for the census data, spatial coverage is thus also very representative for the whole Amazon region. In contrast the lower end of the intermediate range is covered by data from a 114 and a 53 ha plot[13] in Tapajós National Forest and with LiDAR data[14] from southern Peru (Madre de Dios region). Thus the observations of the intermediate range are spatially biased (Fig. 1b,c).

Uncertainties to be addressed with a range of scenarios are thus due to:
(1) *Spatial coverage*. As mentioned above, in contrast to small scale and largest scale disturbances LiDAR data[14] covering a substantial part of the intermediate range are only from one part of Western Amazonia and cover only part of the intermediate range. *We address this with a scenario whereby we assume the disturbance size distribution of the intermediate range to be the one obtained when combining the LiDAR data from terra firme and floodplains, a dramatic and instructive although unrealistic case;*

(2) *Methodological issues*. For forest censuses these include uncertainties in allometries which are quite minor in the big picture (see Feldpausch et al. 2012[53]); a main issue with LiDAR data is the question how long a gap (or disturbance) is detectable by LiDAR. *We address this issue by running our simulator assuming either (a) a detectability time of 1 year or (b) a detectability time of 3.6 year respectively. The 3.6 years are chosen based on long-term observation of gap closure in 50 ha plot of Barro Colorado Island from Hubbell and Foster 1986*[40]. Gap closure varies regionally as data from French Guiana suggest half-lives of small forest gaps in excess of 5 years[41]. The 1 year detectability scenario is thus probably biologically unrealistic.

(3) *Dependence of disturbance size frequency distribution on our given data sample*. We have calculated the uncertainties associated with calculating histograms formally and uncertainties are mostly not large with exception of the largest scales; *we analyse the effect of this source of uncertainty with the following scenarios: (a) assumption of occurrence of largest scale disturbances throughout the region (i.e. not just in the Central Amazon), (b) the standard – in our view most likely case - and (c) omission of largest blow-downs altogether across the entire region.* In light of extensive available data from two studies over two separate time periods using different analysis methods[5,6], we assert that both the full region disturbance and no disturbance scenarios are exceptionally improbable.

(4) *Dependence on observed growth statistics based on RAINFOR forest censuses*. We address this by centering growth (G) around the Amazon region mean of 2.50 Mg C ha^{-1}

yr^{-1} and alternatively the Western Amazon region mean of 2.75 Mg C ha^{-1} yr^{-1} (see Gloor et al., 2009[12]); and

(5) *Central Amazonia (where largest blow-downs are concentrated) versus rest of the Amazon region.* To address this issue we use the same scenarios as described under (3).

The results of the various simulation scenarios are summarized in Table 1 (see main manuscript for more details) and Table S2 (an extreme scenario that assumes the largest blow-downs occurring not only in Central Amazonia but throughout the Amazon regions and intermediate disturbances occurring at a rate that greatly over-represents the importance of floodplain forests). Sample trajectories for a range of scenarios are shown in figure S11 below.

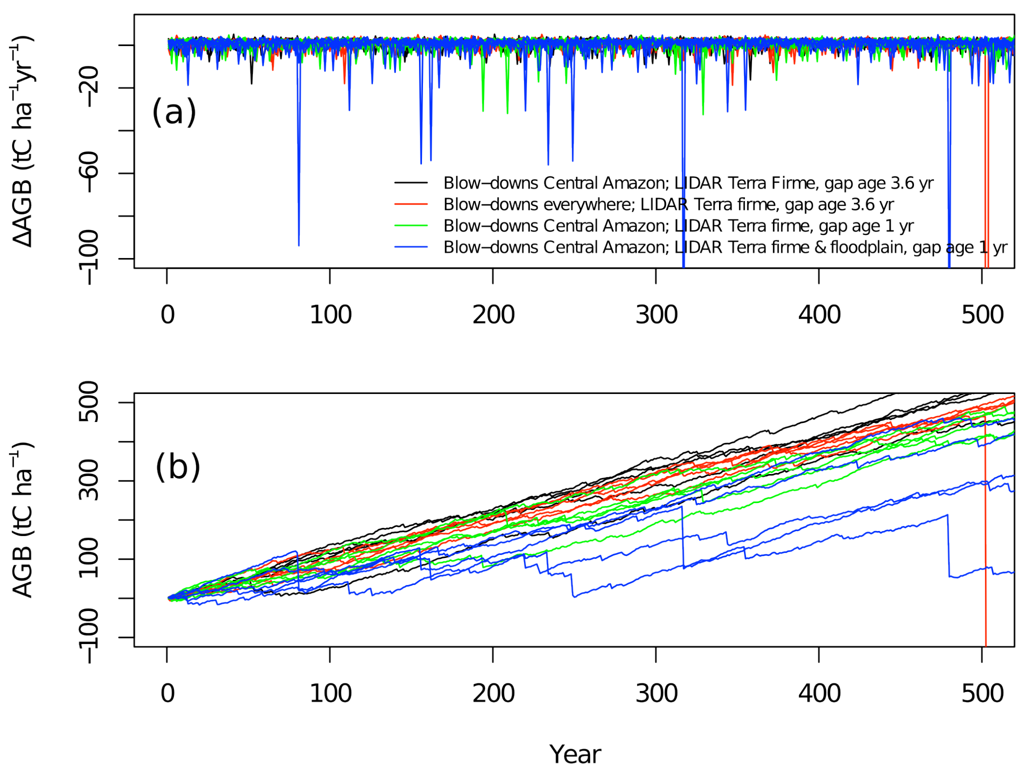

Supplementary Figure S11. *Simulations of the Amazon aboveground biomass change.* Simulations using the full frequency distribution of natural disturbance (small, intermediate and large-scale disturbances) assuming several scenarios of blow-downs occurrence and ages of tree-fall gaps from LiDAR images. Prediction examples of (a) the mean mass balance ΔAGB for annual time-steps and (b) mass balance trajectory of $AGB(year = N) = \sum_{i=1}^{N} \Delta AGB(i)$ for a few members of the sample are presented.

Table S2. Summary of Amazon forest simulator results and statistical significance of simulated mean aboveground biomass gains for a range of extreme scenarios. We analyze three cases of large-disturbance blow-downs[5,6], (the large-end tail of the disturbance frequency distribution): observed (*i*) no large disturbance events , (*ii*) only in central Amazon (~20% of the Amazon region), (*iii*) everywhere in the Amazon with the same frequency of events as in the Central Amazon (i.e. in total there are 5 times more large-area events). For intermediate-range disturbances occurring across the entire Amazon region distributed according to LiDAR surveys[14] (plots 1,4,5 and 12) of depositional-floodplain (DFP) forests (15,178 ha) we assumed an extreme case of a mean gap age of only 1 year. We also assumed an annual mean mass gains[12,18,36] of 2.75 Mg C ha^{-1} yr^{-1}. The simulator of forest mortality is based on the frequency distribution of disturbance area. To convert area losses to biomass losses we assumed a forest mass density of 170 Mg C ha^{-1} for all simulations, a high value and nearly 50% greater than the LiDAR landscape used to estimated intermediate disturbance dynamics[18,36]. Assessment of each scenario is based on a set of 10^9 annual equivalent samples. Significance is assessed with a *t*-test considering $t_{sim} = (dM/dt)/(\sigma/\mathrm{sqrt}(N))$ where *dM/dt* is ensemble mean mass gain, σ the standard deviation of the mass gain distribution and *N* the number of observations. For *N* we use either conservatively $N = 135$ the total number of observational plots or $N = 1545$, the total number of plot census years reflecting the stochastic nature of disturbance and therefore the near independence of plot results from year-to-year. Gain results are statistically significant at the 95% level if $t_{sim} \gtrsim t_{\{0.975,N=135\}} \approx t_{\{0.975,N=1545\}} = 1.96$ and at the 99% level if $t_{sim} \gtrsim t_{\{0.995,N=135\}} \approx t_{\{0.995,N=1545\}} = 2.58$.

Assumed annual mean mass gains[12,18,36]: 2.75 Mg C ha^{-1} yr^{-1} and intermediate-scale disturbances[30,31] modeled with:

Intermediate-Scale Disturbances	Large-Scale Blow-downs[5,6]		
LiDAR data[14] from terra firme and floodplains (gaps age[40] ~ 1 yr old)	None	Central Amazon	All Amazon Region
dM/dt*	0.66	0.66	0.65
σ*	9.76	10.89	14.68
t_{obs}(N=135)	0.79	0.70	0.51
t_{obs}(N=1545)	2.65	2.38	1.74

Supplementary References

1. Whitmore, T. C. Canopy gaps and the two major groups of forest trees. *Ecology* **70,** 536–538 (1989).

2. Brokaw, N. V. L. The definition of treefall gap and its effect on measures of forest dynamics. *Biotropica* **14,** 158–160 (1982).

3. Fraver, S., Brokaw, N. V. L. & Smith, A. P. Delimiting the gap phase in the growth cycle of a Panamanian forest. *Journal of Tropical Ecology* **14,** 673–681 (1998).

4. Van der Meer, P. J., Bongers, F., Chatrou, L. & Riera, B. Defining Canopy Gaps In A Tropical Rain-forest - Effects On Gap Size and Turnover Time. *Acta Oecologica - International Journal of Ecology* **15,** 701–714 (1994).

5. Nelson, B. W. *et al.* Forest disturbance by large blowdowns in the Brazilian Amazon. *Ecology* **75,** 853–858 (1994).

6. Espírito-Santo, F. D. B. *et al.* Storm intensity and old-growth forest disturbances in the Amazon region. *Geophysical Research Letters* **37,** L11403 (2010).

7. Garstang, M., White, S., Shugart, H. H. & Halverson, J. Convective cloud downdrafts as the cause of large blowdowns in the Amazon rainforest. *Meteorology and Atmospheric Physics* **67,** 199–212 (1998).

8. Chambers, J. Q. *et al.* Hyperspectral remote detection of niche partitioning among canopy trees driven by blowdown gap disturbances in the Central Amazon. *Oecologia* **160,** 107–117 (2009).

9. Malhi, Y. *et al.* An International Network to Monitor the Structure, Composition and Dynamics of Amazonian Forests (Rainfor). *Journal of Vegetation Science* **13,** 439–450 (2002).

10. Phillips, O. L. *et al.* Changes in the carbon balance of tropical forests: evidence from long-term plots. *Science* **282,** 439–442 (1998).

11. Phillips, O. L. & Gentry, A. H. Increasing turnover through time in tropical forests. *Science* **263,** 954–958 (1994).

12. Gloor, M. *et al.* Does the disturbance hypothesis explain the biomass increase in basin-wide Amazon forest plot data? *Global Change Biology* **15,** 2418–2430 (2009).

13. Espírito-Santo, F. D. B. *et al.* Gap formation in large forest plots of Brazilian Amazon: Effects on carbon cycling and measurement using high resolution optical remote sensing. *Plant Ecology and Diversity* (2013). doi:10.1080/17550874.2013.795629

14. Asner, G. P. *et al.* Forest Canopy Gap Distributions in the Southern Peruvian Amazon. *PLoS ONE* **8,** e60875 (2013).

15. Phillips, O. L., Lewis, S. L., Baker, T. R., Chao, K. J. & Higuchi, N. The changing Amazon forest. *Philosophical Transactions of the Royal Society B-biological Sciences* **363,** 1819–1827 (2008).

16. Malhi, Y. *et al.* The regional variation of aboveground live biomass in old-growth Amazonian forests. *Global Change Biology* **12,** 1107–1138 (2006).

17. Baker, T. R. *et al.* Variation in wood density determines spatial patterns in Amazonian forest biomass. *Global Change Biology* **10,** 545–562 (2004).

18. Lewis, S. L. *et al.* Increasing carbon storage in intact African tropical forests. *Nature* **457,** 1003–U3 (2009).

19. Chave, J. *et al.* Assessing evidence for a pervasive alteration in tropical tree communities. *PLoS Biology* **6,** e45 (2008).

20. Pyle, E. H. *et al.* Dynamics of carbon, biomass, and structure in two Amazonian forests. *Journal of Geophysical Research* **113,** G00B08 (2008).

21. Chambers, J. Q., Santos, J., Ribeiro, R. J. & Higuchi, N. Tree damage, allometric relationships, and above-ground net primary production in central Amazon forest. *Forest Ecology and Management* **152,** 73–84 (2001).

22. Malhi, Y. *et al.* The above-ground coarse wood productivity of 104 Neotropical forest plots. *Global Change Biology* **10,** 563–591 (2004).

23. Frolking, S. *et al.* Forest disturbance and recovery: A general review in the context of spaceborne remote sensing of impacts on aboveground biomass and canopy structure. *Journal of Geophysical Research-biogeosciences* **114,** G00E02 (2009).

24. Runkle, J. R. Gap Regeneration In Some Old-growth Forests of the Eastern-united-states. *Ecology* **62,** 1041–1051 (1981).

25. Brown, S. *Estimating biomass and biomass change of tropical forests: a primer*. (Food and Agriculture Organization of the United Nations (FAO), Rome, Italy, 1997).

26. Harmon, M. E., Whigham, D. F., Sexton, J. & Olmsted, I. Decomposition and Mass of Woody Detritus In the Dry Tropical Forests of the Northeastern Yucatan Peninsula, Mexico. *Biotropica* **27,** 305–316 (1995).

27. Keller, M., Palace, M., Asner, G., Pereira, R. & Silva, J. N. Coarse woody debris in undisturbed and logged forests in the eastern Brazilian Amazon. *Global Change Biology* **10,** p784–795 (2004).

28. Palace, M., Keller, M., Asner, G. P., Silva, J. N. M. & Passos, C. Necromass in undisturbed and logged forests in the Brazilian Amazon. *Forest Ecology Management* **238,** 309–318 (2007).

29. Palace, M., Keller, M. & Silva, H. Necromass Production: Studies in Undisturbed and Logged Amazon Forests. *Ecological Applications* **18,** 873–884 (2008).

30. Chambers, J. Q., Negrón-Juárez, R. I., and Hurtt, G. C., Marra, D. M. & Higuchi, N. Lack of intermediate-scale disturbance data prevents robust extrapolation of plot-level tree mortality rates for old-growth tropical forests. *Ecology Letters* **12,** E22–E25 (2009).

31. Lloyd, J., Gloor, E. U. & Lewis, S. L. Are the dynamics of tropical forests dominated by large and rare disturbance events? *Ecology Letters* **12,** E19–E21 (2009).

32. Means, J. E. *et al.* Use of large-footprint scanning airborne lidar to estimate forest stand characteristics in the Western Cascades of Oregon. *Remote Sensing of Environment* **67,** 298–308 (1999).

33. Kellner, J. R. & Asner, G. P. Convergent structural responses of tropical forests to diverse disturbance regimes. *Ecology Letters* **12,** 887–897 (2009).

34. Boyd, D. S., Hill, R. A., Hopkinson, C. & Baker, T. R. Landscape-scale forest disturbance regimes in southern Peruvian Amazonia. *Ecological Applications* — (2013). doi:10.1890/12-0371.1

35. Asner, G. P. *et al.* Carnegie Airborne Observatory: in-flight fusion of hyperspectral imaging and waveform light detection and ranging (wLiDAR) for three-dimensional studies of ecosystems. *Journal of Applied Remote Sensing* **1,** 1–21 (2007).

36. Phillips, O. L. *et al.* Drought Sensitivity of the Amazon Rainforest. *Science* **323,** 1344–1347 (2009).

37. Chazdon, R. L. & Pearcy, R. W. The Importance of Sunflecks For Forest Understory Plants - Photosynthetic Machinery Appears Adapted To Brief, Unpredictable Periods of Radiation. *Bioscience* **41,** 760–766 (1991).

38. Phillips, O. L. *et al.* Pattern and process in Amazon tree turnover, 1976–2001. *Philosophical Transactions of the Royal Society: Biological Science* **359 ,** 477–491 (2004).

39. Galbraith, D. *et al.* Residence times of woody biomass in tropical forests. *Plant Ecology & Diversity* **6,** 139–157 (2013).

40. Hubbell, S. P. & Foster., R. B. in *Plant Ecology* (Crawley, M.) 77–95 (Blackwell, Oxford, UK, 1986).

41. Van der Meer, P. J. & Bongers, F. Formation and closure of canopy gaps in the rain forest at Nouragues, French Guiana. *Vegetatio* **126,** 167–179 (1996).

42. INPE. *Instituto Nacional de Pesquisas Espaciais, PRODES (Projeto de Desflorestamento da Amazônia)*. (2011).

43. Tardin, A. T. *et al. Levantamento de areas de desmatamento na Amazônia legal através de imagens do satélite Landsat*. **Inpe-1411-,** 14 (Instituto Nacional de Pesquisas Espaciais, 1979).

44. Shimabukuro, Y. E. & Smith, J. A. The least-squares mixing models to generate fraction images derived from remote sensing multispectral data. *IEEE Transactions on Geoscience and Remote Sensing* **29,** 16–20 (1991).

45. Ter Steege, H. *et al.* Continental-scale patterns of canopy tree composition and function across Amazonia. *Nature* **443,** 444–447 (2006).

46. Ripley, B. D. *Spatial statistics*. 132 (John Wiley & Sons, 1981).

47. Baddeley, A. & Turner, R. spatstat: An R Package for Analyzing Spatial Point Patterns. *Journal of Statistical Software* **6,** 1–42 (2005).

48. Houghton, R. A. Aboveground Forest Biomass and the Global Carbon Balance. *Global Change Biology* **11,** 945–958 (2005).

49. Schimel, D. S. *et al.* Recent Patterns and Mechanisms of Carbon Exchange by Terrestrial Ecosystems. *Nature* **414,** 169–172 (2001).

50. Saatchi, S. S., Houghton, R. A., Alvala, R. C. D. S., Soares, J. V & Yu, Y. Distribution of aboveground live biomass in the Amazon basin. *Global Change Biology* **13,** 816–837 (2007).

51. Negrón-Juárez, R. I. *et al.* Widespread Amazon forest tree mortality from a single cross-basin squall line event. *Geophysical Research Letters* **37,** L16701 (2010).

52. Fisher, J., Hurtt, G., Thomas, Q. R. & Chambers, J. C. Clustered disturbances lead to bias in large-scale estimates based on forest sample plots. *Ecology Letters* **11,** 554–563 (2008).

53. Feldpausch, T. R. *et al.* Tree height integrated into pan-tropical forest biomass estimates. *Biogeosciences* **9 ,** 3381–3403 (2012).